Russian Chemical Reviews **77** (1) 1 – 19 (2008) © 2008 Russian Academy of Sciences and Turpion Ltd

DOI 10.1070/RC2008v077n01ABEH003746

Chemical aspects of the design of thermoelectric materials

A V Shevelkov

Contents

I.	Introduction	1
II.	Fundamentals	2
III.	Traditional thermoelectric materials and their evolution	3
IV.	Phonon glass – electron crystal	6
V.	Disordered semiconductors	9
VI.	Intermetallic compounds	11
VII.	Nanoblock oxides	13
VIII.	Nanosized thermoelectric materials	14
IX.	Conclusion	15

Abstract. The relationship between the composition, structure and properties of promising thermoelectric materials is analysed. Different classes of chemical compounds that serve the basis for the development of thermoelectrics are considered. Special attention is drawn to chemical problems associated with the design of the new-generation thermoelectric materials. The prospects for the development of this research field are demonstrated. The bibliography includes 201 references.

I. Introduction

The resources of fossil fuels are being exhausted as the world's energy consumption increases every year.[1] Such a situation necessitates the development and the use of alternative energy sources. The thermoelectricity phenomenon, which in essence concerns the interconversion of thermal and electrical forms of energy, underlies the development of materials to be used in the generation of power from heat or in the refrigeration under the action of electric current.

Thermoelectric materials, which were discovered back in the 1950s, become more and more important in the power generation, conversion and storage. The constantly increasing attention to the quest for new semiconductors for the thermoelectric refrigeration and power generation is associated with the fact that contemporary 'classical' thermoelectrics based on bismuth and lead tellurides exhibit rather low efficiency. They cannot operate at temperatures below 160 K and their thermoelectric figure-of-merit (ZT) does not exceed 1. Nonetheless, they find practical application in very different fields, from the production of primitive refrigerating bags to modern units designed for either the temperature control or the electricity generation at space stations where the reliability of instruments is valued higher than their cost. Theoretical calculations point to the absence of limitations for the improvement of the thermoelectric figure-of-merit. Hence, new materials should be designed to reach the high efficiency and new methods should be developed for their synthesis.[2, 3]

Thermoelectric power sources will find application in the nearest future; moreover, the main goal is to solve a problem of how to convert the parasitic (waste) heat liberated during the engine operation into electricity. Particularly, it is expected that one can save 20% – 25% of fuel by converting the heat removed from the internal combustion engine of a car into the electric current to be consumed in feeding the car equipment. The use of efficient thermoelectric coolers is extremely advantageous for several reasons. First of all, as compared with conventional compression refrigerating units, thermoelectric devices are very compact and contain no mobile parts, which ensures their high reliability (their service life is 200 000 h, *i.e.*, nearly 25 years); moreover, they do not require any maintenance service. Second, thermoelectric coolers can be integrated into composite devices only one or several parts of which require local cooling. Third, thermoelectric coolers contain no noxious chemicals, which determines their environmental attractiveness. It is expected that on attainment of $ZT = 3$, the efficiency of thermoelectric materials will be sufficient for the general replacement of compression refrigerating devices by thermoelectric units. At the same time, the development of thermoelectric materials capable of operation at low (below 150 K) temperatures will lead to the appearance of a new field of science and technology, namely, superconducting electronics.[4, 5]

The attainment of a high thermoelectric figure-of-merit requires development of semiconductors possessing high electrical conductivity, great thermopower (thermo-emf) and low thermal conductivity. A combination of such properties is rare

A V Shevelkov Department of Chemistry, M V Lomonosov Moscow State University, Leninskie Gory, 119991 Moscow, Russian Federation.
Fax (7-495) 939 47 78, tel. (7-495) 939 12 00,
e-mail: shev@inorg.chem.msu.ru

Received 10 August 2007
Uspekhi Khimii **77** (1) 3 – 21 (2008); translated by T Ya Safonova

and the properties themselves are as a rule closely interrelated, which substantially narrows down the possible scopes of the search for new efficient materials. This is why the problem of finding thermoelectric materials and their optimisation will always be associated with the chemical design, which involves the complex and fine tuning of properties based on the knowledge of the structure – properties relationship for semiconductors and semimetals of different structure and also on the theoretical concepts of solid state chemistry and condensed-matter physics.

This review is devoted to the chemical aspects of the development of new thermoelectric materials. Various trends are considered based on the approaches dominant in modern science. These include the development of the Ioffe classical notions on the thermoelectric properties of 'heavy' semiconductors, the design of thermoelectric materials based on the 'phonon glass – electron crystal' concept and the extension of the latter concept to disordered semiconductors and on the modern ideas on the use of nanostructuring. The evolution of fundamental studies in this field and the prospects for the development of new thermoelectric materials are analysed.

II. Fundamentals

The relationship between electrical current and heat was discovered by Seebeck in 1821. In 1838, Lenz experimentally demonstrated this relationship by passing current through a soldered joint of bismuth and antimony wires, which resulted in freezing of a water drop placed on this joint; the drop melted with the reversal of polarity. The observed phenomenon reflects the interaction between thermal and electrical fluxes. As the measure of this phenomenon, the coefficient of proportionality between a potential difference (ΔV) formed in a non-uniformly heated conductor and a temperature difference between cold and hot ends of the conductor (ΔT) is used, which is called the Seebeck coefficient or thermopower (S)

$$\Delta V = S\Delta T.$$

The Seebeck phenomenon is closely associated with the Peltier effect, *i.e.*, the heat liberation or absorption (depending on the polarity of the applied potential difference) when electrical current is passed through an alloy of two dissimilar conductors. These two effects lie in the basis of operation of thermoelectric refrigerators and power sources.[6]

Figure 1 shows the simplest thermoelectric device. It consists of connected conductors of n- and p-types. When electrical current flows in the direction from the n- to p-conductor, the charge carriers flow away from the working junction and remove heat from it; hence, in accordance with the Peltier law, the working junction is cooled (Fig. 1 *a*). And the other way round, heating of the working element generates an electrical current in the circuit as a result of the same cooperative motion of charge carriers (Fig. 1 *b*). The simplest devices are assembled into compact batteries assembled in series electrically and in parallel thermally. The efficient operation of such a battery depends first of all on the efficiency (figure-of-merit) of the thermoelectric material.[7]

The figure-of-merit of a thermoelectric material is a dimensionless coefficient ZT

$$ZT = S^2T\sigma\kappa^{-1},$$

where T is the absolute temperature, σ is the electrical conductivity of the material, κ is its thermal conductivity. The $S^2\sigma$ product is also referred to as the power factor, because it determines the efficiency of transport of charge carriers. The

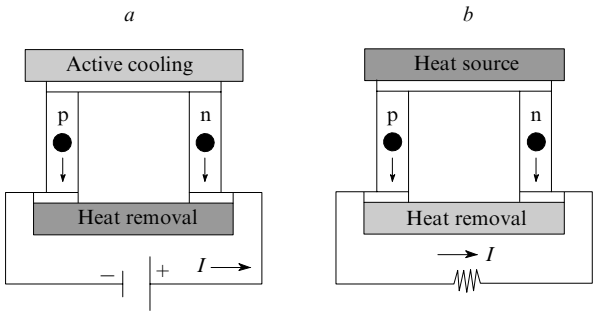


Figure 1. A scheme of the simplest thermoelectric device for (*a*) cooling and (*b*) power generation.

power factor is maximum for doped semiconductors with the charge carrier concentration reaching the orders of magnitude of $10^{19}-10^{20}$ cm^{-3}. This is explained by the fact that, although semiconductors exhibit the lower electrical conductivity as compared with metals, their Seebeck coefficients may be substantially higher. For metals, the Seebeck coefficients rarely exceed $1-5$ μV K^{-1}. In contrast, semiconductors can demonstrate thermopower values that approach $\pm 10^3$ μV K^{-1} at room temperature, where the polarity depends on the sign of predominant carriers, *viz.*, electrons (negative) or holes (positive). Theoretical calculations showed that to reach $ZT = 1$, which corresponds to the highest values for the conventional materials used rather extensively, the Seebeck coefficient should not be lower than 157 μV K^{-1}.

In addition to the high power factor, an effective thermoelectric material should exhibit low thermal conductivity. The thermal conductivity of semiconductors includes two components, namely, the lattice and the electronic contributions, which reflect the propagation of heat in solids by means of phonons and conduction electrons, respectively. The electronic component (κ_e) is related to the electrical conductivity by the following relationship:

$$\kappa_e = L_0\sigma T,$$

where L_0 is the ideal Lorentz number equal to 2.45×10^{-8} V^2 K^{-2}. Hence, an increase in electrical conductivity may lead to an increase in thermal conductivity. It is known that for metals, the contribution of the electronic component into the thermal conductivity may exceed 50%. The lattice component of thermal conductivity is associated with the quantised lattice vibrations, *i.e.*, phonons. This component is the highest for highly symmetrical ordered crystals built of atoms of light elements with small-amplitude temperature vibrations for which the propagation of phonons is the least hindered. The intensification of the phonon scattering and, correspondingly, the reduction of the lattice-type thermal conductivity can be achieved by the increase in the atomic mass and by the formation of heterogeneities, interfaces, or resonance systems. The thermal conductivity of efficient thermoelectric materials should not exceed 2 W m^{-1} K^{-1}.

Preparation of thermoelectric materials requires the use of substances with the high conductivity of the semiconducting type, a high Seebeck coefficient and low, predominantly lattice-type thermal conductivity. For a narrow-gap semiconductor, the combination of a low thermal conductivity with a high electrical conductivity is a rare phenomenon, which limits the choice of candidates for the development of effective thermoelectric materials. Thus, the main problem consists in

the simultaneous optimisation of the mentioned three properties, where the mechanisms that govern the reduction of thermal conductivity and the increase in the power factor should not compensate each other. The next Sections of this review describe different chemical methods of solving this problem.

III. Traditional thermoelectric materials and their evolution

The practical application of the effect of the thermoelectric refrigeration and the reverse effect of thermoelectric power generation was encouraged by the predictions made by A F Ioffe in the mid-1950s.[8] According to his conclusions, the efficient thermoelectic materials should be sought among narrow-gap semiconductors of post-transition elements of the 5th and 6th periods. Such a substance should exhibit a high power factor due to the high concentration of carriers and their large effective mass, and, at the same time, have a relatively low thermal conductivity, because its crystal structure is built of heavy atoms. Studies that had followed this prediction led to the development of a family of thermoelectric converters (transducers) based on doped tellurides of bismuth and lead.[2] These materials were used for half a century without substantial increase in their figure-of-merit.

1. Bismuth and lead tellurides

Bismuth and lead tellurides were the first compounds that provided the basis for thermoelectric materials. These compounds have different crystal structures. Bismuth telluride Bi_2Te_3 has a layered structure of the tetradymite type (Fig. 2). Layers formed by bismuth and tellurium atoms alternate along the *c* axis of the rhombohedral lattice and are joined into blocks each containing five layers. Within a block, atoms are bonded by strong covalent interactions, whereas between blocks, van der Waals forces act. Quite a different structure is typical of PbTe, which is crystallised in the rock salt type. The compound Bi_2Te_3 has a considerable range of homogeneity and, depending on the composition in this range, may exhibit different types of conduction, namely, p or n types.[9] By varying synthetic methods, one can obtain Bi_2Te_3 with the required concentration of carriers of a given type. The thermal conductivity of this telluride is composition-independent. It is strongly anisotropic for a single-crystal bismuth telluride and amounts to ~ 1.9 W m^{-1} K^{-1} for a ceramic sample, which corresponds to $ZT \approx 0.6$ for the optimum compositions within the homogeneity region and for samples with optimum morphology.[10] The addition of antimony or selenium to Bi_2Te_3 made it possible to substantially decrease the thermal conductivity and to obtain ZT close to 1 for the $Bi_2Te_{3-x}Se_x$ and $Bi_{2-x}Sb_xTe_3$ solid solutions (Fig. 3).[11–13] The literature information on the further alloying of solid solutions is conflicting; however, there are no indications of any substantial increase in the thermoelectric figure-of-merit as a result of such alloying.[14, 15] The optimised synthetic methods were used to improve the properties of thermoelectric materials based on bismuth telluride which involved hot pressing, spark plasma sintering and extrusion.[16, 17]

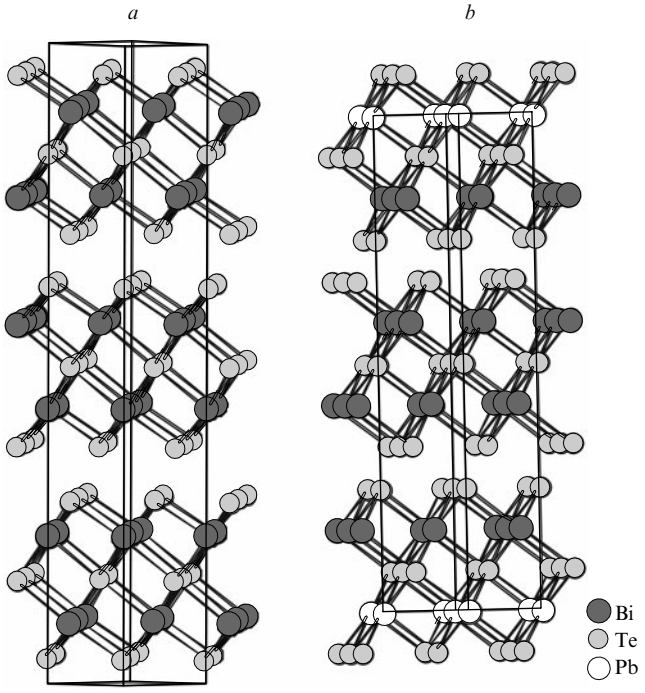


Figure 2. Crystal structures of (*a*) Bi_2Te_3 and (*b*) $PbBi_4Te_7$.

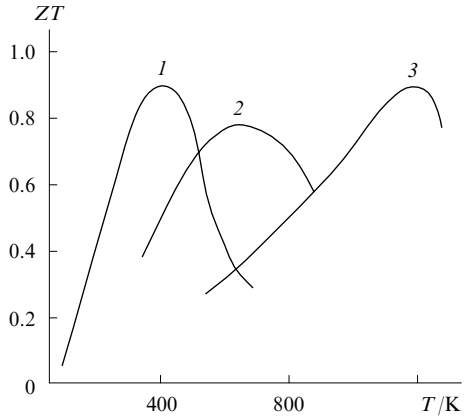


Figure 3. Figure-of-merit of traditional materials as a function of temperature.
(*1*) Bi_2Te_3, (*2*) PbTe, (*3*) $Si_{0.3}Ge_{0.7}$.

The thermoelectric properties of pure lead telluride are of no special interest. However, alloying it with the donor or acceptor additives gave rise to considerable electrical conductivity of the p- or n-type, whereas the formation of the $Pb_xSn_{1-x}Te$ solid solution resulted in a decrease in the thermal conductivity. The Group 13 elements are considered as the most promising; alloying with antimony telluride was also successfully used.[18, 19] At room temperature, the thermoelectric figure-of-merit of alloyed $Pb_xSn_{1-x}Te$ did not exceed 0.1, but as the temperature increased, it reached the maximum $ZT = 0.75$ at $T = 700$ K (see Fig. 3).[20] It was also found that the method of preparation of a ceramic material substantially affects its figure-of-merit.[21, 22] The literature contains information on the 'mutual doping' of Bi_2Te_3 and PbTe. It was found that lead telluride retains its rock-salt structural type upon the introduction of up to 1 mol % of bismuth telluride. It was noted that such alloying simultaneously increased the electronic component and decreased the lattice contribution to the thermal conductivity in such a way that the overall thermal conductivity remained unchanged, whereas the thermopower and the electrical conductivity increased. As a result, the

thermoelectric figure-of-merit doubled at room temperature as compared with pure PbTe.[23]

The properties of thermoelectric materials based on lead telluride and the peculiarities of their application were surveyed in a recent review.[24]

2. Alloys Si – Ge

Alloys Si – Ge, which represent a solid solution Si_xGe_{1-x} from the chemical viewpoint, occupy a special place among the conventional thermoelectric materials.

The elemental silicon and germanium are crystallised in the diamond structural type. Having very rigid and symmetric lattices, they exhibit thermal conductivity too high to become good thermoelectric materials (150 and 63 W m^{-1} K^{-1}, respectively, at room temperature). However, their thermal conductivity can be reduced to approximately 5 – 10 W m^{-1} K^{-1} due to the formation of a solid solution.[25,26] It was shown that the formation of the solid solution neither involves any ordering of silicon and germanium atoms in the crystal structure nor affects the mobilities of charge carriers. The chemical stability of Si_xGe_{1-x} solid solutions at high temperatures, particularly, against oxidation, provides prerequisites for the high-temperature (1000 – 1200 K) use of thermoelectric materials based on them; moreover, their efficiency approached 0.9 for $x \approx 0.3$ (see Fig. 3).[25,27]

Alloys Si – Ge are intended for use at high temperatures; hence, in choosing the alloying agents, the following factors should be borne in mind. First, the resulting alloy should exhibit sufficiently high chemical stability at $T \leqslant 1200$ K; second, the atomic size should not be too large to prevent distortion of the diamond-like structure. Doping of different Si_xGe_{1-x} alloys with boron led to a substantial increase in the thermopower (up to 10^3 μV K^{-1}); however, this did not involve any increase in the figure-of-merit, which was largely due to the decrease in the electrical conductivity.[28]

3. Mixed chalcogenides with complex structures

The development of Ioffe's ideas on the preparation of thermoelectric materials based on narrow-gap semiconductors comprising heavy metals gave rise to an entire series of studies aimed at the search for compounds with more complicated crystal structures (derivatives of the tetradymite structure) among the ternary and quaternary bismuth selenides and tellurides. Virtually all compounds of this kind are narrow-gap semiconductors and exhibit relatively low thermal conductivity. Varying the crystal structures and the constituent chemical elements offers wide possibilities for the optimisation of thermoelectric properties of these materials.

The $PbTe-Bi_2Te_3$ system comprises several compounds[29] the structure of which can be described as the intergrowth of layers along the c axis of a trigonal cell. Among these compounds, of special interest is $PbBi_4Te_7$ with a crystal structure (see Fig. 2) characterised by the complex ordering of layers (parameter $c = 71.7$ Å),[30] which points to its low thermal conductivity. The compound $PbBi_4Te_7$ represents an n-type semiconductor with the concentration of carriers of an order of magnitude of 10^{20} cm^{-3}, which exhibits the high electrical conductivity and thermopower; the thermoelectric figure-of-merit approached the maximum $ZT = 0.5$ at 600 K.[31,32] It was reported that the partial substitution of selenium for tellurium in $PbBi_4Te_7$ causes a decrease in the thermal conductivity and an increase in the thermopower.[33] Isostructural compounds $GeBi_4Te_7$ and $SnBi_4Te_7$ also demonstrated interesting thermoelectric properties, albeit lower figure-of-merit values; however, the maximum ZT values were shifted to low temperatures.[32] Compounds in the Ge – Bi – Te and Sn – Bi – Te systems that had the same structural type but different orders of alternation of blocks in the trigonal cells and the different ordering of dissimilar atoms were described in the literature;[34] however, they ranked below $PbBi_4Te_7$ as regards the thermoelectric properties.

Telluride $CsBi_4Te_6$ exhibited the most promising properties among all mixed chalcogenides.[35] This compound crystallises in a new structural type, which can be represented as the anionic $Bi_4Te_6^-$ layers with a distorted NaCl structure regularly alternating with the layers of Cs^+ cations (Fig. 4). In the $CsBi_4Te_6$ compound, Bi^{2+} and Bi^{3+} formally co-exist in a ratio of 1 : 3; moreover, the analysis of crystal structure suggested that one fourth of bismuth atoms are bound into Bi – Bi pairs (the Bi – Bi distance is 3.24 Å) and that these pairs make a substantial contribution to the low-dimensional anisotropic transport of charge carriers.[36] Pure $CsBi_4Te_6$ is a degenerate p-type semiconductor with a weak negative temperature dependence of conductivity, which was about 4×10^4 S m^{-1} at room temperature; the thermopower was 115 μV K^{-1} at the same temperature. Alloying of $CsBi_4Te_6$ with different substances led to the formation of both n- and p-type materials with the double electrical conductivity and the thermopower reaching 150 μV K^{-1} (Ref. 37). At the same time, the development of more complex compounds based on $CsBi_4Te_6$ by introduction of tin or lead atoms into their structure almost halved their thermopower.[38]

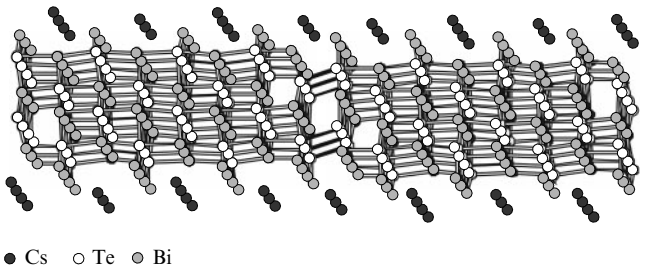


Figure 4. Crystal structure of $CsBi_4Te_6$.

The thermal conductivity of $CsBi_4Te_6$ was within 1.3 – 1.8 W m^{-1} K^{-1} depending on the nature and degree of alloying, which is worse than expected taking into account that this compound is built of heavy atoms and the volume of its unit cell is very large (3250 Å). Apparently, this can be explained by a substantial contribution of the electronic component to thermal conductivity, which is comparable with the phonon component. Nonetheless, in the temperature range of 180 – 250 K, $CsBi_4Te_6$ demonstrated the high thermoelectric figure-of-merit values, namely, varying from 0.4 for the pure compound to 0.8 for a compound with 0.03% SbI_3 (Fig. 5).[37]

It should be noted that nowadays, the alloyed $CsBi_4Te_6$ is the only thermoelectric material capable of operating at low temperatures (down to 150 – 160 K), which is determined by the peculiarities of its band structure, first of all, the degenerate nature of its band gap and the contribution of Bi – Bi dimers into the states near the Fermi level. However, the technological prospects of this material are vague, because its synthesis requires the use of extremely reactive metallic ceasium or its telluride as the starting compound.

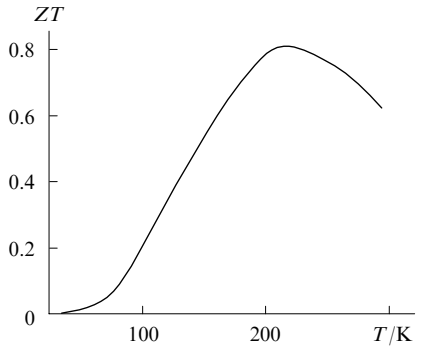


Figure 5. Thermoelectric figure-of-merit of $CsBi_4Te_6$ as a function of temperature.

Among the rest mixed tellurides, mention should be made of a compound $Bi_3Cu_{14-x}Te_{12}$ with a complex, difficult-to-describe structure with the unit cell volume of $\sim$2700 Å^3 (depending on x). As regards its electronic structure, this telluride should be classified with degenerate semiconductors; however, in contrast to $CsBi_4Te_6$, it has low thermopower (about 15 μV K^{-1}); this is why despite its sufficiently low thermal conductivity (0.95 W m^{-1} K^{-1} at 300 K), it exhibited very low thermoelectric figure-of-merit.[39]

Not only mixed tellurides, but also other chalcogenides, namely, sulfides and selenides, were the subjects of studies aimed at the quest for thermoelectric materials, despite the lower atomic masses of selenium and especially sulfur as compared with tellurium. In the general case, the mass reduction leads to an increase in thermal conductivity, which is compensated by the complex structure of sulfides and selenides. It is for selenides that the complex compounds with crystal structures representing different motifs of the intergrowth of blocks with structures of several types were obtained.[40] Among their specific features are anisotropy, low symmetry, the alternation of dissimilar atoms in a single or several crystallographic sites, the presence of weakly bound atoms. The properties of these compounds strongly depend on their composition, *e.g.*, for β-$K_2Bi_{8-x}Sb_xSe_{13}$, the thermopower at 300 K varied from -400 μV K^{-1} for $x = 5.6$ to -120 μV K^{-1} for $x = 2.4$; moreover, the thermal conductivity of mixed selenides only slightly exceeded the values typical of systems based on bismuth telluride.[41]

4. Thallium compounds

In recent years, interest was aroused in thallium compounds as promising thermoelectric materials. This was caused by two factors. First, thallium resembles certain alkali metals as regards chemical and crystallographic properties. It preferentially forms compounds in the oxidation state +1, its ionic radius is very close to that of potassium but its electronegativity is high.[42] The substitution of thallium for potassium may narrow the band gap of a compound as its chemical bond becomes less ionic and thus lead to an increase in the electrical conductivity. Second, thallium is a heavy element; hence, its introduction into semiconductors, particularly, into bismuth and lead tellurides, should decrease their thermal conductivity.

Studies of mixed thallium tellurides have shown that certain representatives of this class of compounds exhibit promising thermoelectric properties. Incorporation of thallium into bismuth telluride allowed quite a number of new compounds to be obtained; their properties were studied.[43] It was found that Tl_9BiTe_6 demonstrates the best thermoelectric properties. It is crystallised in the Tl_5Te_3 structural type.[44,45] In its structure, one can single out a perovskite-like pattern of distorted octahedra formed by tellurium atoms and containing the randomly distributed bismuth and thallium atoms (Fig. 6). The rest thallium atoms are located in the voids between octahedra in such a way that each thallium atom forms only three relatively short (3.1–3.5 Å) bonds with tellurium atoms. The following two specific features of this structure provide the low thermal conductivity: the high content of heavy atoms (the atomic fractions of thallium and bismuth add up to 2/3) and the random alternation of bismuth and thallium atoms in octahedral positions. As a consequence, the thermal conductivity of Tl_9BiTe_6 was only 0.4 W m^{-1} K^{-1} at room temperature, the maximum thermoelectric figure-of-merit of 0.89 was reached at 580 K; the use of conductivity-enhancing alloying made it possible to reach $ZT = 1.2$ at 500 K.[46–48]

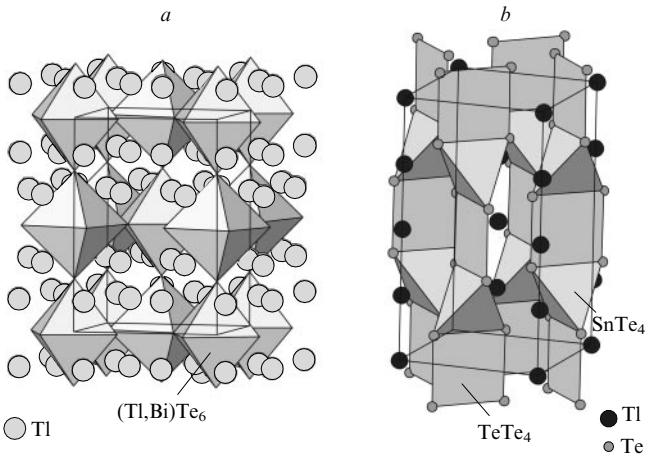


Figure 6. Crystal structures of (*a*) Tl_9BiTe_6 and (*b*) Tl_2SnTe_5.

By now, the thermoelectric properties of a large number of thallium-containing compounds were studied.[44,48–54] They had different values of figure-of-merit but all exhibited low thermal conductivities (Fig. 7), as a rule, below 1 W m^{-1} K^{-1}. It was found that the lowest thermal conductivity (0.2–0.3 W m^{-1} K^{-1}) is typical of phases in the Ag–Tl–Te system, where a high thermoelectric figure-of-merit value reaching 1.23 at 700 K was observed for Ag_9TlTe_5.[49,50] The compound Tl_2SnTe_5 demonstrated a somewhat lower figure-of-merit ($ZT = 1$ at 500 K).[44] It is of interest that the crystal structures of these compounds did not resemble that of Tl_9BiTe_6. Moreover, the structural fragments were also different. Thus the structure of Ag_9TlTe_5 should be considered as a derivative of the Ag_2Te structure, whereas in Tl_2SnTe_5, the main structural building block is a $SnTeTe_4$ chain in which tin atoms are surrounded by tetrahedra of tellurium atoms. Some tellurium atoms are in a positive oxidation state and are surrounded by squares of tellurium atoms in a negative oxidation state (see Fig. 6). It is assumed that the key role in the provision of low thermal conductivity is played by thallium, namely, its large atomic mass, the peculiarities of its asymmetric position in the crystal structure with the typically not-too-high coordination numbers and the corresponding asymmetric temperature vibrations. However, the low thermal conductivity is not always accompanied by high power factors. Thus, as regards its structural properties, namely, the presence of the conducting 3D framework and of

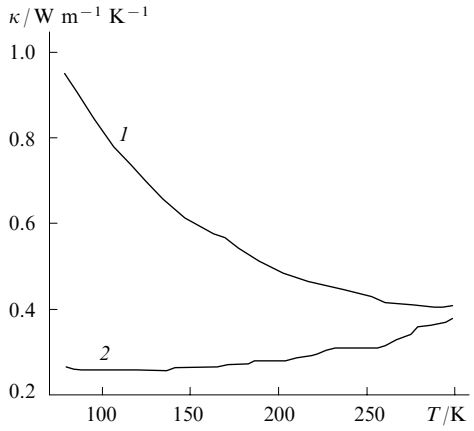


Figure 7. Thermal conductivity of thallium-containing semiconductors as a function of temperature.
(*1*) $Tl_2CdSnTe_4$, (*2*) $Tl_2Cu_2SnTe_4$.

thallium atoms asymmetrically located in tunnels, the compound $Tl_2Cu_2SnTe_4$ should demonstrate promising thermoelectric properties. However, according to measurements, its electrical conductivity did not exceed 0.1 S m^{-1}, which led to very low values of ZT.[51]

It should be noted that thallium is very toxic. Nonetheless, the discovery of effective thermoelectric materials among thallium compounds is of great significance, insofar as designing and studying substances with the high values of figure-of-merit makes it possible to retrieve information on the structure – property relationship.

IV. Phonon glass – electron crystal

The resumed interest in the design of fundamentally new thermoelectric materials was associated with the development and primary evaluation of new theoretical concepts, of which the Slack idea on the development of a substance that is a good electrical conductor (like a crystal) but a bad thermal conductor (like glass) is of the greatest importance.[55] According to the original idea, an effective thermoelectric material should be sought among substances that contain weakly bound atoms (or molecules) capable of free rotation or oscillation within a limited volume (the so-called rattlers). Such rattlers would effectively scatter phonons thus decreasing the thermal conductivity, but would not have any substantial effect on the electrical conductivity provided by a framework bound by covalent chemical bonds of low polarity. Thus, there appears a possibility to independently optimise the thermal conductivity and the transport of charge carriers, which raises the probability of developing a material with the high thermoelectric figure-of-merit.[5, 7, 55]

1. Filled skutterudites

Filled skutterudites have become the first subjects studied within the frames of a concept 'phonon glass — electron crystal' (PGEC). This family owes its name to a mineral skutterudite with the chemical composition $CoAs_3$. In the skutterudite crystal structure, cobalt atoms form a primitive cubic lattice, while arsenic atoms combined into planar anions As_4^{4-} occupy the positions in six of the eight octants. Two octants in the skutterudite crystal structure are vacant; however, a family of compounds is known in which the octants are occupied by large cations of electropositive metals (Fig. 8).

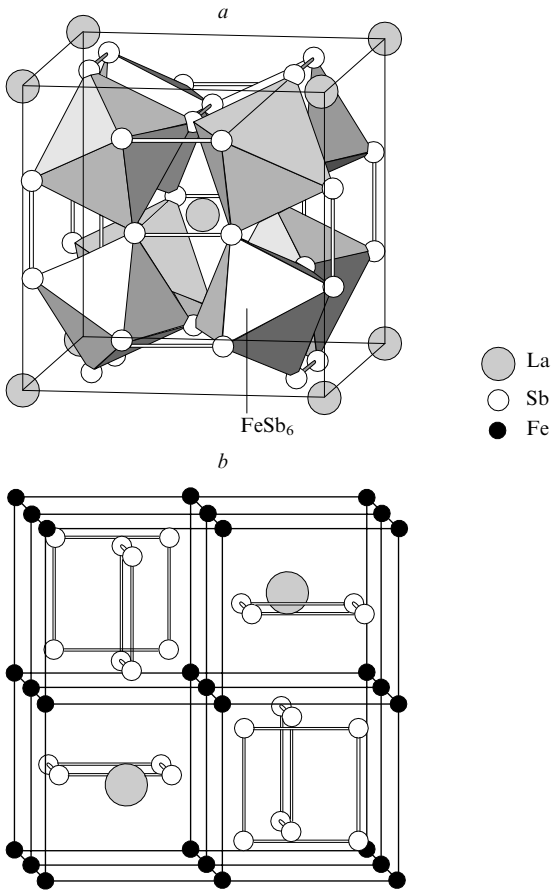


Figure 8. Crystal structure of a filled skutterudite.
(*a*) Arrangement of $FeSb_6$ octahedra and La^{3+} cations in a unit cell; (*b*) primitive cubic packing formed by iron atoms, octant-forming Sb_4^{4-} anions and La^{3+} cations (the cell is shifted by 1/4, 1/4, 1/4).

Such compounds are described by the general formula $A_xT_4E_{12}$, where A is an alkali, alkaline-earth, or, less often, rare-earth metal, indium or tin, T is a transition metal of Group 8 or 9 and E is phosphorus, arsenic, or antimony. They are traditionally called 'filled skutterudites', while the cations are referred to as 'fillers' or 'guest atoms'.[56–58]

Filled skutterudites represent a reasonable subject for studying thermoelectric properties in the framework of the PGEC concept. The filler atoms are located in large cages formed by 12 atoms of a Group 15 element and have large atomic displacement parameters, which makes possible the effective phonon scattering. Their interactions with atoms of the skutterudite framework are preferentially of the ionic nature; hence, their effect on the electronic properties of a compound is weak. At the same time, the transition-metal atoms each surrounded by an octahedron formed by Group 15 atoms are always in the low-spin ground state, and the levels in the vicinity of the Fermi level preferentially consist of the non-metal molecular π-orbitals, which determines the transport of charge carriers in filled skutterudites (Fig. 9).[59, 60]

The diversity of chemical properties of filler metals and of transition metals that form the framework offers rich possibilities for varying the electronic properties of these compounds. Skutterudites-antimonides attract the keenest attention due to their ability to form the largest cavities that allow the filler atoms to oscillate with greater amplitudes; moreover, antimonides demonstrate the better electronic conductivity as com-

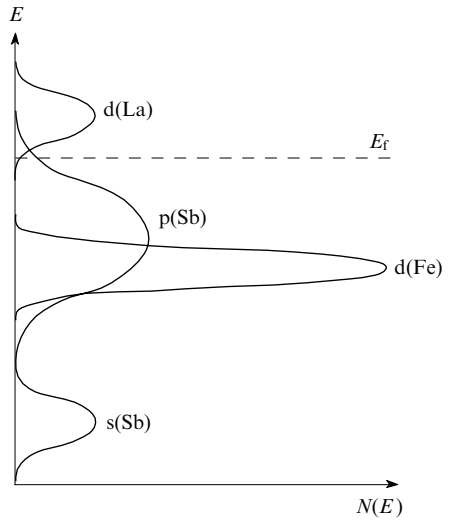


Figure 9. Band structure of the filled skutterudite $LaFe_4Sb_{12}$. The distribution of the density of state [$N(E)$] over energy is shown (E_f is the Fermi level).

pared with arsenides and phosphides. It was found that slutterudites-antimonides can exhibit both n- and p-conduction. A combination of high electrical conductivity, large thermopower and low thermal conductivity led to very high figure-of-merit values for these compounds. Thus for $LnFe_3CoSb_{12}$ (Ln = La, Ce), $ZT = 1.4$ for temperatures about 1100 K (Fig. 10).[61,62] As a rule, with a decrease in the guest atom size and mass, the phonons are scattered more effectively and, correspondingly, the thermal conductivity decreases. However, the incomplete occupancy of guest positions may introduce the additional dynamic or static disordering,[63] which favours a more pronounced decrease in the thermal conductivity of a filled skutterudite.[64–66]

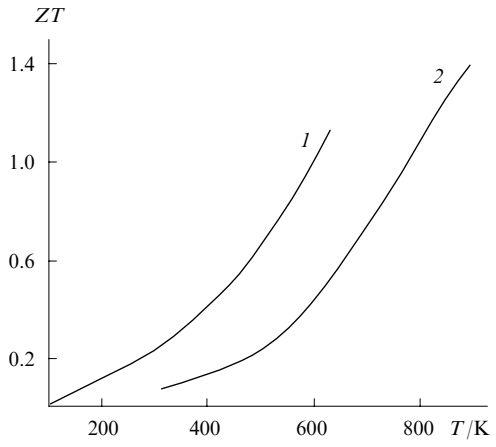


Figure 10. Thermoelectric figure-of-merit of filled skutterudites as a function of temperature.
(*1*) $Yb_{0.19}Fe_4Sb_{12}$, (*2*) $CeFe_3CoSb_{12}$.

The transport of charge carriers through a skutterudite framework also considerably depends on the nature of a guest metal that plays the role of the electron donor. Based on the data of X-ray electron spectroscopy, the atoms of $LaFe_4P_{12}$ were assigned to the following oxidation states:[67] $(La^{3+})(Fe^{2+})_4(P^-)_{12}$; hence, the filled skutterudite represents a non-valence electron-deficient compound. Irrespective of whether the assignment of the oxidation states was correct, it is possible to claim that because the non-metal molecular π-orbitals make the largest contribution to the states near the Fermi level, there arises a possibility of varying the valence states *via* the heterovalent substitutions without affecting the semiconductor type of conduction. It should also be borne in mind that the oxidation state of a transition metal may change. For example, in $NaFe_4Sb_{12}$, the d^5 and d^6 centres (Fe^{3+} and Fe^{2+}) became ferromagnetically ordered,[68] a more sophisticated magnetic interaction was observed in $GdRu_4P_{12}$.[69] Heterovalent substitutions may result in the appearance of high (up to 10^{21} cm^{-3}) concentrations of charge carriers.[62] Thus the substitution of nickel for a small part of cobalt atoms in $Ba_xCo_4Sb_{12}$ increased its thermoelectric figure-of-merit almost 1.5-fold.[70] The electron density concentration donated by a guest atom also plays a substantial role; moreover, with the exception of low temperatures (up to 200 K), the f-orbitals of rare-earth guest atoms do not contribute to the thermoelectric properties of filled skutterudites. By the example of $Yb_xCo_4Sb_{12}$, it was shown that the thermal conductivity weakly varies with the composition for low ytterbium contents, whereas the changes in electronic conductivity and thermopower led to doubling of the thermoelectric figure-of-merit, *viz*., from $ZT = 0.6$ for $x = 0.07$ to $ZT = 1.2$ for $x = 0.12$ at 800 K.[65] In contrast, the introduction of a small amount of tin into $CoSb_3$ led to the appearance of the metal-type conduction, although the thermal conductivity substantially decreased as compared to the unfilled compound and reached the minimum for $Sn_{0.25}CoSb_3$.[71]

The studies of thermoelectric properties of common (*i.e*., unfilled) skutterudites were also carried out, being stimulated by their high electrical conductivities and thermopowers. For example, for $CoGe_{1.5}Te_{1.5}$ in which the ordering of tellurium and germanium atoms results in their lower, rhombohedral symmetry, the Zeebeck coefficient was found to be -697 μV K^{-1} at 273 K,[72] whereas for $IrSn_{1.5}Te_{1.5}$ with the same superstructure type, the thermopower did not exceed 160 μV K^{-1} under the same conditions and only weakly depended on the substitution of rhodium or palladium for iridium and also of indium for tin.[73] However, the thermal conductivity of common skutterudites turned out to be too high, exceeding 10 W m^{-1} K^{-1} (Ref. 74), which is an order of magnitude higher than the values observed for filled skutterudites. This fact stresses that a specific mechanism of scattering of heat-carrying phonons by concerted vibrations of guest atoms is realised in filled skutterudites.

2. Semiconducting clathrates

Clathrates form a vast family of compounds characterised by the great diversity of crystal structures. In addition to ordinary clathrates (gas hydrates), several families of semiconducting compounds are known to crystallise in one of five types of clathrate structures.[75] The promising thermoelectric properties are typical of compounds with the clathrate-I structure (Fig. 11). The crystal structure of clathrates is based on four-bonded networks composed of atoms of one or several elements of Groups 13, 14 or 15, where only the presence of a Group 14 element is mandatory (the only exclusion[76] is $Ba_8Cu_{16}P_{30}$). The networks (or frameworks) surround large cavities occupied by guest atoms, namely, cations (of alkali and alkaline-earth metals or europium) or anions (halides or tellurides). Depending on the nature of the guest atom,

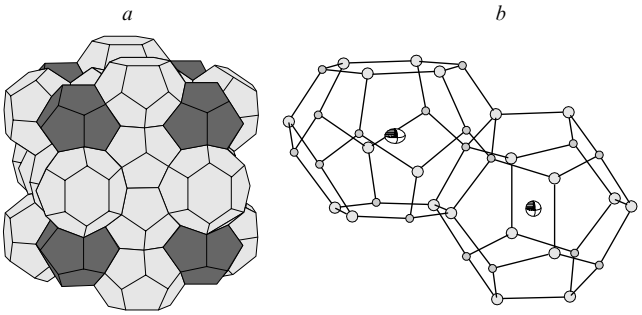


Figure 11. Crystal structure of clathrate-I.
(*a*) Polyhedral representation, (*b*) 20- and 24-vertex polyhedra adjacent at the common pentagonal face with embedded guest atoms.

clathrates are divided into cationic and anionic. A cationic clathrate has a positively charged framework with a halogen or tellurium atom playing the role of the guest, whereas an anionic clathrate has a negatively charged framework and an electropositive metal as the guest atom. The general composition of compounds with the clathrate-I structure is written as $A_8[E_{46}]$, *i.e.*, their cubic unit cell contains 8 guest atoms per 46 framework atoms.[77,78]

The specific features of the clathrate crystal structures are responsible for their anomalously low thermal conductivity comparable with that of glasses. Guest atoms trapped in large cavities and surrounded by 20 or 24 framework atoms are capable of rattling in the available space thus scattering heat-carrying phonons. The resulting thermal conductivity depends on the following factors: the guest-atom size and mass, the 'guest–host' size matching and the possibility that the guest atoms of different kind alternated in the framework cages. In the general case, the thermal conductivity decreases as the guest atom mass and the volume free for its oscillations increase, and with the increase in the degree of disordering in the distribution of two different 'guests'. For the majority of clathrates, the thermal conductivity at room temperature was lower than 1 W m^{-1} K^{-1} and for certain compounds, *e.g.*, $[Sn_{24}P_{19.3}]Br_2I_6$, it dropped below 0.5 W m^{-1} K^{-1} (Fig. 12).[79–83]

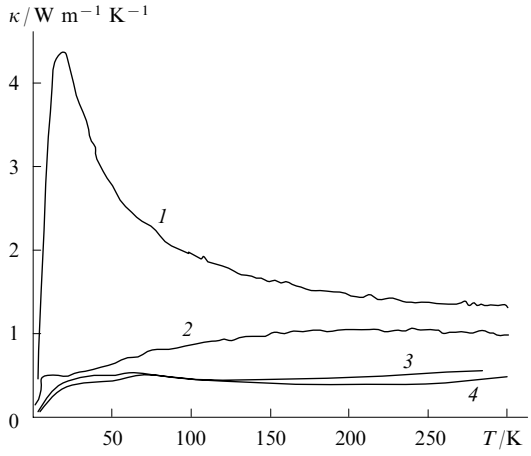


Figure 12. Temperature dependences of thermal conductivity of certain semiconducting clathrates.
(*1*) $Ba_8Ga_{16}Ge_{30}$, (*2*) $Sr_8Ga_{16}Ge_{30}$, (*3*) $Sn_{24}P_{19.3}Br_2I_6$, (*4*) $Sn_{20.5}As_{22}I_8$.

For the majority of clathrates, a decrease in the temperature led to a slight decrease in the thermal conductivity, which corresponded to a decrease in the amplitude of guest atom oscillations.[84,85] This confirms that clathrates exhibit the phonon glass properties, because it is glasses (and amorphous substances, in general) that feature the phonon scattering, the latter representing the atomic oscillation waves on structural irregularities.[6] The localised nature of guest atom oscillations is manifested in the temperature dependence of the heat capacity from which the Einstein temperature can be determined. The latter corresponds to the characteristic vibrational frequencies of guest atoms in a given compound and lies in a range of 50–120 K depending on the guest atom. The low-temperature segment of the temperature dependence of thermal conductivity cannot be described as merely the scattering by guest-atom oscillations; two additional possible mechanisms are considered, namely, the lattice relaxation and the tunnelling of a guest atom trapped in a large cavity over several neighbouring positions.[81,86] The thermal conductivity also depends on the lattice disordering. Thus the thermal conductivity of a disordered clathrate $[Sn_{20.5}As_{22}]I_8$ is only 0.45 W m^{-1} K^{-1}, which is almost twice as low as that of its much better ordered analogues $[Sn_{24}P_{19.3}]X_8$ (X = Br, I).[79,87,88]

The 'guest–host' interaction in clathrates is usually described as electrostatic.[89,90] 'Guest' atoms are substantially ionised, they donate (being electropositive metals) or accept (halogens or tellurium) electrons to allow all framework atoms to complete an electron octet by forming the two-electron two-centred homonuclear and heteronuclear bonds and, if necessary, lone electron pairs. As a consequence, most of clathrates exhibit semiconducting properties and their composition—structure relationship is described in terms of the Zintl concept for valence compounds.[91,92]

According to calculations, the actual electronic structure of clathrates is very complicated despite all the simplicity of its qualitative description. It substantially depends on the chemical identity of atoms that form the compound.[93,94] Clathrates described by the Zintl scheme are narrow-gap semiconductors; moreover, the vacancies predicted by this scheme play an important role because the main contribution to the states in vicinity to the Fermi level is made by the orbitals of vacancy-adjoining three-coordinated atoms with a lone pair or by the orbitals of heteroatoms.[90,95] By regulating the concentration of vacancies and performing different substitutions in the clathrate framework, it is possible to vary the density of states near the Fermi level, which is reflected in the local electronic environment of atoms and, for tin-based clathrates, was confirmed by Mössbauer spectra.[96] Hence, clathrates offer wide possibilities in tuning the electronic structure and, correspondingly, properties by performing different substitutions in the framework aimed at the change in the charge-carrier concentration and its effective mass. As a result of such substitutions, it is possible to synthesise compounds with the electrical conductivity varying from several tens to 10^5 S m^{-1}, while the thermopower of n-type conductors can reach -800 μV K^{-1} at room temperature.[80,97] Nonetheless, the best thermoelectric figure-of-merit at 300 K was merely 0.4 for $Eu_8Ga_{16-x}Ge_{30+x}$, while at 870 K, $ZT = 0.87$ for $Ba_8Ga_{16}Si_{30}$.[98,99]

Clathrates of the different structural types were also studied as the candidates for thermoelectric materials. First of all, this concerns compounds of the clathrate-II type, which are distinguished by the incomplete occupancy of guest positions by atoms of alkali or alkaline-earth metals.[100,101] The changes in the occupancy lie in the basis of fine tuning of transport

properties. It was shown that caesium and a part of sodium atoms may be removed from the compound $Na_8Cs_{16}Si_{136}$ with the clathrate-II structure, which led to a five-orders-of magnitude decrease in the electrical conductivity and a 20-fold decrease in the thermal conductivity; however, the thermoelectric figure-of-merit of the best samples did not exceed 0.05.[100]

V. Disordered semiconductors

The development of the PGEC concept gave rise to new ideas in the preparation of phonon glasses based on narrow-gap semiconductors. It was assumed that the lattice irregularities, namely, the alternation of chemical elements with different masses in one crystallographic position or the disordering of atoms of one or more elements over several neighbouring positions, are responsible for the efficient phonon scattering.[102, 103] The effect of a disordering on the thermal conductivity was already mentioned in this review by the example of $Sn_{20.5}As_{22}I_8$;[79] however, the main subjects of studies in terms of a new view on the PGEC concept turned out to be Zn_4Sb_3 and its analogues and compounds of the LAST family, which are described in the next two Sections.

1. Compounds of the LAST family

Compounds of the LAST family represent mixed tellurides of silver, lead and antimony of the general composition $AgPb_mSbTe_{m+2}$ (their name LAST is the abbreviation of English names of elements, *i.e.*, lead – antimony – silver – tellurium). The quantity m can vary from zero to infinity, insofar as these compounds represent the unlimited solid solution in the $AgSbTe_2-PbTe$ system with the NaCl structure. In this structure, tellurium atoms occupy the positions of chlorine ions, whereas silver, lead and antimony atoms are disordered and randomly alternate in the sodium-ion positions.[104] The contents of different elements in the LAST family compounds is always such that its any member is a valence compound, because the anion charge is always $2-$ (Te^{2-}) and the molar fractions of silver and antimony are equal to one another; hence, the average cation charge is $2+$.

The random distribution of three types of atoms with different masses over the lattice positions of one kind is responsible for the effective phonon scattering and, hence, the decrease in thermal conductivity. For different m, the compounds $AgPb_mSbTe_{m+2}$ demonstrated close values of thermal conductivity, namely, below 0.5 W m^{-1} K^{-1} at 700 K and $\sim$1.3 W m^{-1} K^{-1} at room temperature. All compounds of the LAST family exhibit semiconductor properties with the band gap of $\sim$0.25 eV. The electrical conductivity of compounds increases with an increase in m, reaching 2×10^5 S m^{-1} for $m = 18$. Electrons are the predominant charge carriers; hence, the Zeebeck coefficient is negative and falls in the range from -135 to -335 μV K^{-1} (Ref. 104).

For the LAST compounds enriched in tellurium and lead ($m > 16$), it is possible to synthesise specimens with low silver content and composition corresponding to $Ag_{1-x}Pb_mSbTe_{m+2}$. This was shown to be accompanied by a non-monotonic increase in the thermal conductivity of samples and a simultaneous decrease in their thermoelectric figure-of-merit, namely, the maximum value $ZT = 0.33$ was observed at 673 K for $Ag_{1-x}Pb_{18}SbTe_{20}$ ($x \approx 0.3$) and $ZT = 1.07$ $Ag_{0.6}Pb_{18}SbTe_{20}$ (Refs 105 and 106). However, the concomitant partial substitution of bismuth atoms for lead atoms have led to a substantial increase in the power factor, which was associated with a considerable increase in the electrical conductivity but the Zeebeck coefficient remained virtually invariant.[104] The literature also contains information on the substitution of tin atoms for a part of lead atoms in the LAST compounds; however, this caused no improvement in their thermoelectric properties.[107]

The good conducting characteristics and the high power factor of the LAST family compounds is explained by the appearance of resonance states in the lower part of the conduction band and in the upper part of the valence band. These states can be represented as modified $Te-Ag(Sb)$ bonds formed as a result of substitution of an equivalent number of silver and antimony atoms for a part of lead atoms in lead telluride, which is accompanied by the lowering of the lattice symmetry.[108] Nonetheless, the increase in the power factor is small as compared with the values typical of pure lead telluride; hence, the good thermoelectric figure-of-merit values for the LAST compounds were largely determined by the effective decrease in their thermal conductivity (Fig. 13).[109]

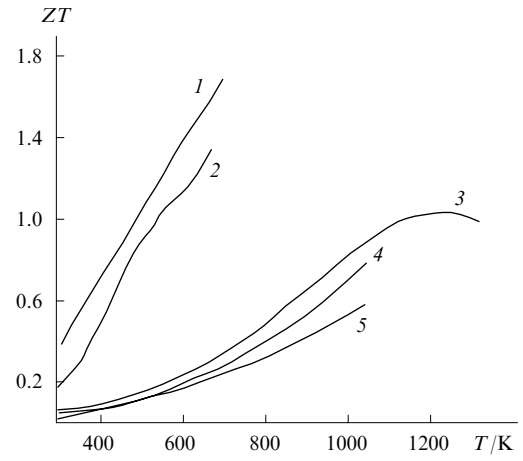


Figure 13. Thermoelectric figure-of-merit of certain disordered semiconductors and intermetallics as a function of temperature.
(*1*) $AgPb_{18}SbTe_{20}$, (*2*) Zn_4Sb_3, (*3*) $Yb_{14}MnSb_{11}$, (*4*) $Mo_3Sb_{5.4}Te_{1.6}$, (*5*) $Mo_3Sb_{5.5}Te_{1.5}$.

According to recent studies, the reasons for the high thermoelectric figure-of-merit of the Last family compounds may be associated with their specific phase heterogeneity. Although, according to X-ray diffraction data, bulk $Ag_{1-x}Pb_mSbTe_{m+2}$ specimens with m from 6 to 18 are single-phase, the results of electron diffraction and high-resolution electron microscopy suggest that different microscopic phases co-exist in these specimens. These phases differ in compositions. It is always possible to single out the main, lead-enriched phase and a set of microphases enriched in antimony and silver. Each microphase has lower symmetry, namely, tetragonal or rhombohedral. In all the cases, it is possible to observe regions of the ordered alternation of antimony, lead and silver atoms. Thus, the question arises of whether the statement that a solid solution $AgSbTe_2-PbTe$ exists is true.[110] However, the observed tetragonal or rhombohedral distortion corresponds to the already mentioned calculations, which demonstrated that the high power factor is associated with the lowering of the symmetry.[109]

It was reported that silver atoms in the LAST family compounds could be completely displaced by sodium atoms with the preservation of high thermoelectric properties. Partic-

ularly, $Na_{0.95}Pb_{20}SbTe_{22}$ demonstrated $ZT = 1$ at 475 K and $ZT = 1.7$ at 700 K. It was shown that such high values of figure-of-merit were largely due to the low thermal conductivity caused by the high degree of lattice disordering. Thus the thermal conductivity was equal to ~ 0.8 W m^{-1} K^{-1} for the same composition $Na_{0.95}Pb_{20}SbTe_{22}$ at 700 K.[111]

From the formal viewpoint, bearing in mind the structural similarity, compounds of the $AgSbTe_2-GeTe$ system are related to the LAST family. These compounds demonstrate relatively high thermoelectric figure-of-merit values. At 700 K, ZT reached 1.2 for the $(AgSbTe_2)_{0.85}(GeTe)_{0.15}$ composition; however, the thermal stability of these compounds was low, and heating to 700 K caused a phase transition followed by a partial mass loss.[112, 113]

2. Zinc antimonide

Zinc antimonide Zn_4Sb_3 has several crystalline modifications, of which only one, β-Zn_4Sb_3, has a considerable degree of disordering and is of prime interest as a candidate for thermoelectric materials for medium-temperature applications. The β-phase exists in a temperature range of 260–765 K; above this temperature, the γ-modification that decomposes to ZnSb and Zn on slight heating is formed and below 260 K, the α- and α′-modifications exist.[114, 115] The β-Zn_4Sb_3 antimonide crystallises in the rhombohedral space group $R\bar{3}c$. In its structure (Fig. 14), one can single out octahedra of zinc atoms that encage antimony atoms joined in pairs with a distance of 2.82 Å. Between the octahedra, there are antimony atoms that do not form Sb–Sb bonds being only bound to zinc atoms. The positions of antimony atoms are completely filled, whereas the positions of zinc atoms at octahedra vertices are filled by roughly 90%; moreover, three additional scarcely populated positions exist which house extra zinc atom. Taking into account the degrees of occupancy, the β-Zn_4Sb_3 composition should be rewritten as $Zn_{3.6}Sb_3$ or $Zn_{11.9}Sb_{10}$.[103, 114, 116] The latter formula allows one to compare the structures of the α- and β-forms. The low-temperature form turns out to have a monoclinic structure, which contains only one additional completely occupied zinc position. This modification corresponds to a chemical composition $Zn_{13}Sb_{10}$. Yet another low-temperature modification, Zn_4Sb_3, named the α′-phase is formed on cooling of the α-form due to the lowering of symmetry to triclinic.[117, 118] Thus, the phase transition $\alpha' \rightarrow \alpha \rightarrow \beta$ described in the literature as reversible actually represents a process accompanied by stoichiometry variations due to the zinc evolution on the transition from α-Zn_4Sb_3 to β-Zn_4Sb_3.[114]

The high thermoelectric figure-of-merit that exclusively belongs to β-Zn_4Sb_3 is related in many ways to the considerably lower thermal conductivity due to the structural disordering and the appearance of the relevant phonon-glass property. Indeed, containing no heavy metals or rattlers, this phase exhibits a thermal conductivity of about 0.9 W m^{-1} K^{-1} at room temperature. Presumably, the principal mechanism of phonon scattering consists of their interactions with randomly located zinc atoms with thermal vibrations of large amplitudes.[116]

Antimonide β-Zn_4Sb_3 is also characterised by a relatively high power factor with the maximum of 1.35×10^{-3} W m^{-1} K^{-2}. The crystallographic analysis showed that α-Zn_4Sb_3 is the only valence compound, whereas for β-Zn_4Sb_3 one must expect the manifestation of metallic properties. Indeed, taking into account the peculiarities of atomic coordination, the composition of the α-modification

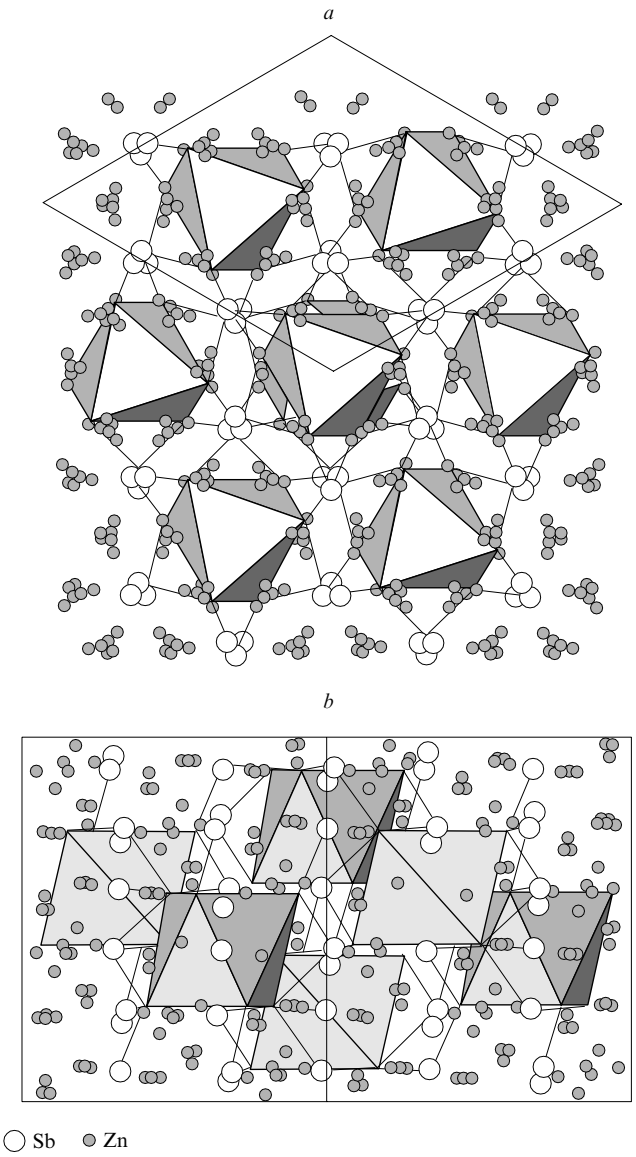


Figure 14. Crystal structure of β-Zn_4Sb_3.
(*a*) View along *c* axis, (*b*) projection on the $(\bar{1}10)$ plane. Octahedra Sb_2Zn_6 are presented as polyhedra.

can be written as $(Zn^{2+})_{13}(Sb_2^{4-})_2(Sb^{3-})_6$, *i.e.*, all bonding states should be occupied and all antibonding states should be vacant. The β-modification is characterised by the deficiency of zinc atoms; hence, the appearance of uncompensated charge carriers should be expected. The experimental and theoretical studies of the band structure have shown that the α-phase is a semiconductor with the band gap of 0.2–0.3 eV.[117, 119] The electronic structure of β-Zn_4Sb_3 is much more complicated. It is possible to rationalise this structure by outlining the Zn_2Sb_2 fragments with a four-centred four-electron bond that involves the sp^3-hybrid orbitals of zinc and antimony atoms (Fig. 15). Based on calculations, it was concluded[119, 120] that the disordered zinc atoms play the role of electron donors and their concentration determines the gap opening at the Fermi level to give rise to the p-type conduction. Moreover, it was shown that the same zinc atoms determine the complex form of the Fermi surface, which is responsible for the high thermopower values.[119, 120]

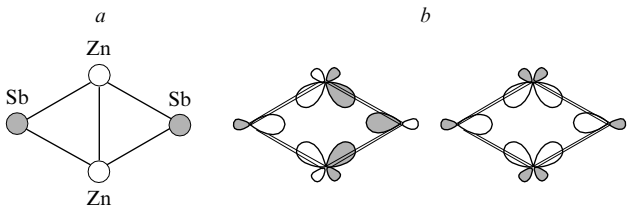


Figure 15. (*a*) A Zn_2Sb_2 fragment of the Zn_4Sb_3 crystal structure and (*b*) two four-centred bonding orbitals therein.

It was found that the thermoelectric figure-of-merit of β-Zn_4Sb_3 reached the maximum $ZT = 1.4$ at 675 K, which makes this substance the most suitable candidate for medium-temperature applications (see Fig. 13).[102] However, a trend of zinc antimonide to contain admixed oxygen-containing phases can be confirmed by the literature data. Depending on the oxygen content, ZT varied from 0.93 for samples with low oxygen contents to 1.08 for samples with 0.625 mass % oxygen at 620 – 660 K. It was noted that the oxygen content differently affects the components of thermoelectric figure-of-merit. The power factor was the highest for samples with the lowest oxygen contents, whereas the thermal conductivity substantially decreased with the increasing oxygen content.[121]

The alloying of β-Zn_4Sb_3 with bismuth, tin and indium did not lead to higher figure-of-merit values.[114, 116] Unexpected results were obtained in the studies of the Zn_4Sb_3 interaction with its cadmium analogue. The compound Cd_4Sb_3 is formally isostructural to β-Zn_4Sb_3, albeit written as a more complex distribution of extra cadmium atoms over the crystal structure. Moreover, for Cd_4Sb_3, no polymorphous transformations were revealed.[122 – 124] The mutual solubility of β-Zn_4Sb_3 and Cd_4Sb_3 was limited and did not exceed 6 mol % of cadmium antimonide at 675 K but increased at higher temperature; the maximum attainable composition was $Zn_{3.1}Cd_{0.9}Sb_3$. A partial substitution of cadmium for zinc always had an adverse effect on the thermoelectric figure-of-merit. This could be due to the fact that Cd_4Sb_3 exhibits the metal conduction.[122, 125, 126] The complex and insufficiently clear crystal and electron structures of β-Zn_4Sb_3 obscure the ways to the further optimisation of its thermoelectric figure-of-merit.

VI. Intermetallic compounds

Most alloys and intermetallic compounds exhibit very high electrical conductivities, but, like metals, have low Zeebeck coefficients (usually, in the range of 1 – 5 μV K^{-1}). Nonetheless, intermetallics are known for which at a certain concentration of valence electrons, a gap is open at the Fermi level, which leads to a substantial increase in the thermopower; moreover, their high electrical conductivity may be retained. Complex crystal structures with large-volume unit cells or with randomly alternating atoms of different masses may have relatively low thermal conductivity. Such properties are typical of several families of compounds, which include several true intermetallic compounds (*e.g.*, semi-Heussler alloys) and polar intermetallics (of which most contain antimony and pertain to the Zintl phases).[91, 127]

1. Semi-Heussler alloys

Semi-Heussler alloys form a large group of intermetallic compounds crystallised in the structural type of MgAgAs. The cubic lattice of MgAgAs can be represented as a derivative of the sphalerite structure with vacant tetrahedral voids that trap extra atoms. Thus, the atoms of one kind (As in MgAgAs) acquire the cubic environment.[128] Semi-Heussler alloys are formed by many chemical elements. The peculiarity of their structure is such that, having from 8 to 18 valence electrons (per formula unit), they exhibit semiconductor properties even if they incorporate only metals. For example, TiNiSn possesses 18 valence electrons and has a band gap of 0.3 eV.[129]

Semiconductor compounds of the family of semi-Heussler alloys attract attention as the promising thermoelectric materials. Here charge transfer occurs as a result of hybridisation of orbitals. Thus in ZrNiSn, d-orbitals of zirconium and nickel atoms strongly interact with one another but virtually do not interact with p-orbitals of tin atoms with lower energies. As a result, a gap at the Fermi level is open, which corresponds to the formal atomic charges $Zr^{4+}Ni^0Sn^{4-}$ (Refs 130, 131). Such compounds demonstrated high electrical conductivity (up to 10^5 S m^{-1}) for relatively high thermopower values; hence, high power factors are reached (about 0.02 W m^{-1} K^{-2} at 400 K). However, owing to their simple and ordered crystal structure, the semi-Heussler alloys inevitably exhibit rather high thermal conductivity (20 – 50 W m^{-1} K^{-1}) and, correspondingly, a low thermoelectric figure-of-merit.[132, 133] To enhance this value, mixed doping was used, which simultaneously decreased the thermal conductivity due to the mass variation and increased the thermopower due to the lesser compensation of charge carriers. Particularly, $ZrNiSn_{0.98}Sb_{0.02}$ demonstrated $ZT = 0.28$ at 573 K; for $(Zr_{0.7}Hf_{0.3})_{0.7}Ti_{0.3}NiSn$ at 800 K, $ZT = 0.32$. The figure-of-merit noticeably increased with the partial substitution of palladium for nickel and reached $ZT = 0.7$ at 800 K for a composition $Hf_{0.5}Zr_{0.5}Ni_{0.8}Pd_{0.2}Sn_{0.99}Sb_{0.01}$.[134 – 136]

2. Polar intermetallics

Promising thermoelectric properties at high temperatures were observed for an intermetallic compound $Yb_{14}MnSb_{11}$ characterised by a high chemical stability. It crystallises in the $Ca_{14}AlSb_{11}$ structural type to form a complex structure, which comprises $[MnSb_4]$ tetrahedra with the formal charge 10 –, linear hypervalent anions Sb_3^{7-}, Sb^{3-} anions (present in a ratio 1 : 2 : 1) and Yb^{2+} cations (Fig. 16 *a*).[137] This compound exhibits the properties of a semimetal or a 'bad' metal, because its electrical conductivity decreases from 5×10^4 S m^{-1} at 300 K to 2×10^4 S m^{-1} at 1200 K, while the thermopower remains high (50 – 200 μV K^{-1}). According to the magnetic and X-ray electron measurements, ytterbium and manganese are in the oxidation states +2. Insofar as the total charge of antimony atoms is −29, the compound contains uncompensated charge carriers at a concentration of 1.3×10^{21} cm^{-3}. Thermal conductivity of $Yb_{14}MnSb_{11}$ is relatively low, which is typical of a complex crystal structure with a unit cell volume of ~6300 $Å^3$, namely, 7 W m^{-1} K^{-1} at 300 K and 9 W m^{-1} K^{-1} at 1200 K; moreover at high temperatures, the contribution of the electronic component exceeds 70%. The thermoelectric figure-of-merit of $Yb_{14}MnSb_{11}$ was merely 0.2 at room temperature, but substantially increased with increasing temperature to reach the maximum $ZT = 1.0$ at 1223 K (see Fig. 13).[138 – 140] To date, $Yb_{14}MnSb_{11}$ has the highest thermoelectric figure-of-merit at high (above 900 K) temperatures.

The unlimited solid solution $Ca_xYb_{1-x}Zn_2Sb_2$ has a structure, which can be described as a pattern formed by layers with the modified zinc blend (ZnSb) structure; between the layers,

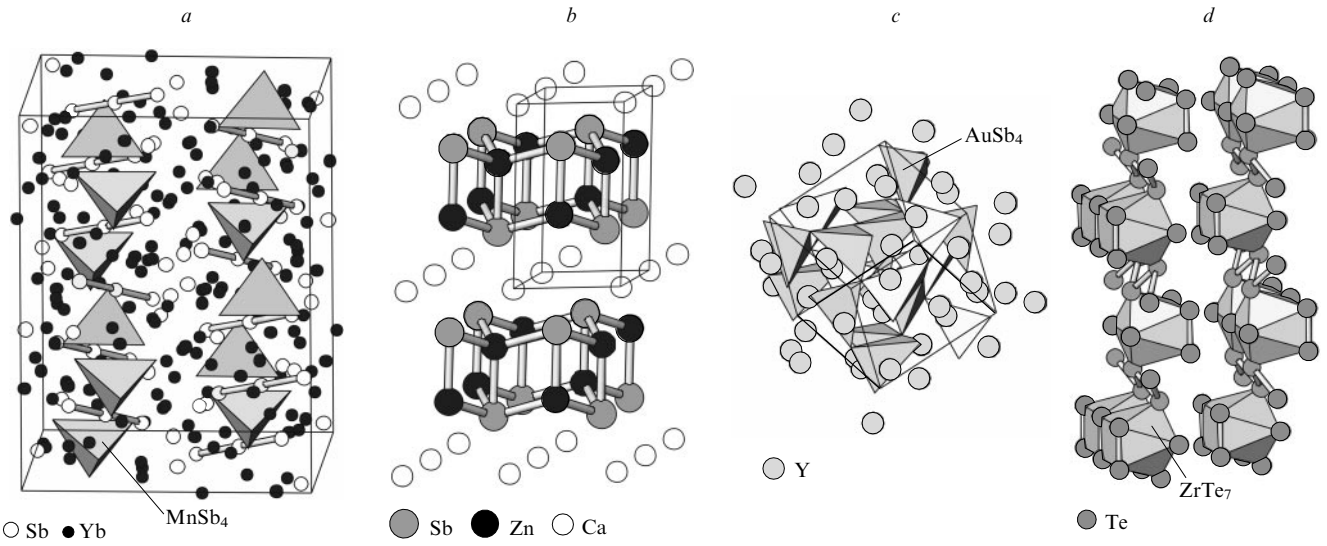


Figure 16. The structures of certain polar intermetallics. (*a*) $Yb_{14}MnSb_{11}$, (*b*) $CaZn_2Sb_2$, (*c*) $Y_3Au_3Sb_4$ (*d*) $ZrTe_5$.

randomly alternating Ca^{2+} and Yb^{2+} cations are located (Fig. 16*b*).[141, 142] Varying the solid solution composition, it is possible to vary many parameters. For example, the concentration of charge carriers increases with an increase in the ytterbium content due to the less pronounced transfer of the electron density from a cation to a two-dimensional anion $Zn_2Sb_2^{2-}$. At the same time, the minimum thermal conductivity was reached for the composition $Ca_{0.5}Yb_{0.5}Zn_2Sb_2$, which was explained by the optimal mixing of calcium and ytterbium possessing different atomic masses. Finally, the highest thermopower values are typical of the calcium derivative ($x = 1$). A combination of these three parameters is such that the highest thermoelectric figure-of-merit was observed for $Ca_{0.25}Yb_{0.75}Zn_2Sb_2$, namely, $ZT = 0.55$ at 800 K.[143]

High thermopower values were observed for certain intermetallic compounds of the general composition $A_3T_3E_4$, where A is an f- or d-element with a large atomic radius, T is a transition metal of group 9–11, E is Sb or Bi. The structure of these compounds is derived from the Th_3P_4 structure *via* the ordered filling of vacant tetrahedral voids in the distorted body-centred packing of the Group 15 atoms (Fig. 16*c*).[144] These intermetallics exhibited semiconductor properties and demonstrated high thermopower values if the number of valence electrons per formula unit was 62, which is typical of such phases as $Zr_3Ni_3Sb_4$ or $Sm_3Au_3Sb_4$.[145, 146] The latter compound is known by the weak dependence of its electrical conductivity on the temperature; the assessed band gap was merely 0.36 meV. The optimisation of $Sm_3Au_3Sb_4$ properties through the formation of a small number of vacancies and substitution of neodymium atoms for samarium provided the thermopowers of about 200 μV K^{-1} and the thermal conductivities below 2 W m^{-1} K^{-1} (Refs 147 and 148).

The concentration of valence electrons determines the properties of compounds with the general composition T_3E_7, where T is a transition metal of Group 5–10, E is a post-transition metal of Group 13–15. These compounds crystallise in the structural type of Ir_3Ge_7 and have a very complex structure that consists of interpenetrating frameworks, where the main building block is an archimedean antiprism doubled along its square base, *i.e.* T_2E_{12}.[149] The number of valence electrons in the T_3E_7 compounds is 51–56; however, the semiconductor properties are manifested only for $55e^-$ per formula unit. This is associated with a gap opened in the band structure, which separates the bonding and antibonding d–p-interactions T–E.[150] Thus $Nb_3Sb_2Te_5$ and $Mo_3Sb_{7-x}Te_x$ ($x \approx 2$) exhibit semiconductor properties. Minor deviations from 55 are possible; in this case, the required concentration of charge carriers is achieved, thus optimising the thermoelectric properties. For $Mo_3Sb_{5.4}Te_{1.6}$, the figure-of-merit value was 0.8 at 1000 K (see Fig. 13).[151, 152]

Low-dimensional pentatellurides $ZrTe_5$ and $HfTe_5$ with the structures somewhat resembling that of Bi_2Te_3 (Fig. 16*d*) were also studied. Bearing in mind the peculiarities of chemical bonds in these compounds, the MTe_5 crystal structure can be described as chains built of trigonal prisms MTe_3 that are further bound by tellurium atoms into layers; between the layers, van der Waals forces operate.[153] Zirconium and hafnium atoms are in the formal oxidation states +4 and play the role of electropositive cations, whereas tellurium atoms form a polyanionic structure typical of the Zintl phases. Pentatellurides MTe_5 demonstrated an unusual resistive transition at temperatures about 100 K (Fig. 17); their Zeebeck coefficient was about −125 μV K^{-1} in the transition point and about +120 μV K^{-1} at room temperature. The nature of the resis-

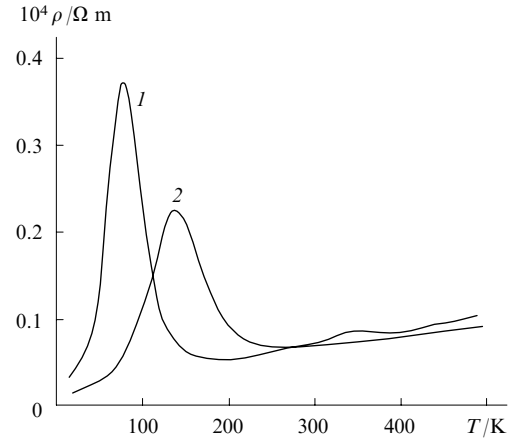


Figure 17. Anomaly of resistive properties of (*1*) $HfTe_5$ and (*2*) $ZrTe_5$.

tive transition is unclear; however, it was shown that the effect disappears upon doping with antimony up to the composition $MTe_{4.75}Sb_{0.25}$ in this case, the metallic conduction was observed in the whole range from 10 to 300 K. The further substitution of antimony atoms for tellurium is apparently impossible due to the formation of ZrSbTe and HfSbTe compounds that have the NbPS-type structures, the metal-type conductivity and a low thermopower.[154] Compounds MTe_5 demonstrated high power factors (up to 7.5×10^{-3} W m^{-1} K^{-2} in the temperature range of 150–250 K), which suggests that these compounds can be used in low-temperature devices. Nonetheless, their properties require further optimisation, insofar as unalloyed pentatellurides exhibited relatively high thermal conductivities [above 4 W m^{-1} K^{-1} (Refs 155 and 156)].

3. Kondo intermetallics

In contrast to most metals, intermetallic compounds of f-elements with the variable oxidation states may exhibit high thermopower values due to the manifestation of the Kondo effect. This effect (or the Kondo resonance) is the result of interaction of 4f-electrons localised on an atom with the conduction electrons. This results in a very high density of states near the Fermi level, which leads to the appearance of high thermopower with retention of the metal-type conduction. As a rule, the Kondo effect is typical of Ce and Yb compounds, although it was observed for other lanthanides and even actinides.[157, 158]

Among metallic conductors, the high thermopower values were observed for the intermetallics $YbAl_3$ and $CePd_3$ with simple crystal structures of the $CuAu_3$ type. The thermopower reached its maximum at temperatures near 200 K and was equal to -80 μV K^{-1} for $YbAl_3$ and $+125$ μV K^{-1} for $CePd_3$. The different signs of thermopower suggest that in the Kondo intermetallics, both electrons and holes may serve as the dominant charge carriers. Taking into account the high electrical conductivity, the power factor can reach very large values, for example, its maximum value for $YbAl_3$ was about 0.03 W m^{-1} K^{-2}. Nonetheless, these compounds exhibit low thermoelectric figure-of-merit (ZT did not exceed 0.2) due to their high thermopower values caused by the large contribution of the electronic component and the simplicity of their symmetric crystal structure.[159, 160]

It should be noted that the Kondo effect is manifested by certain cerium derivatives with the structure of $Y_3Au_3Sb_4$ discussed in the previous Section. Thus the compound $Ce_3Pt_3Sb_4$ demonstrated metallic conduction (its electrical conductivity was $\sim 10^5$ S m^{-1} at room temperature) but had a high thermopower value, which could be increased to 300 μV K^{-1} (the peak at 120 K) by changing a part of cerium atoms for neodymium. Nonetheless, due to the high thermal conductivity, the maximum value of the thermoelectric figure-of-merit did not exceed 0.12.[161]

VII. Nanoblock oxides

The number of oxide thermoelectric materials is few, because compounds with the low thermal conductivity are scarce among binary and complex semiconducting oxides. At the same time, the evident advantage of oxide thermoelectrics is their resistance to oxidation; they can serve the basis for the development of materials capable of the thermoelectric power generation at high temperatures. To transform mixed oxides into the potential thermoelectrics, a concept of nanoblock assembling of crystalline structures was used according to which blocks responsible for either the high electrical conductivity or the low thermal conductivity alternated along one of the lattice directions. The applicability of this approach was first demonstrated for $NaCo_2O_4$, which, as was shown later, represents one of compositions of the Na_xCoO_2 phase ($0.3 \leqslant x \leqslant 1$).[162, 163] In the crystal structure of this compound (Fig. 18), the layers built of condensed CoO_2 octahedra alternate with layers of Na^+ cations. The transport properties of $NaCo_2O_4$ measured on a single crystal pointed to the strong anisotropy of its electrical conductivity. The resistance along CoO_2 layers was very low (2×10^{-6} Ω m), while its temperature dependence pointed to the metallic nature of conduction. In the same plane, the thermopower value was 100 μV K^{-1} at room temperature, which is an order of magnitude higher than the values typical of metals.[164]

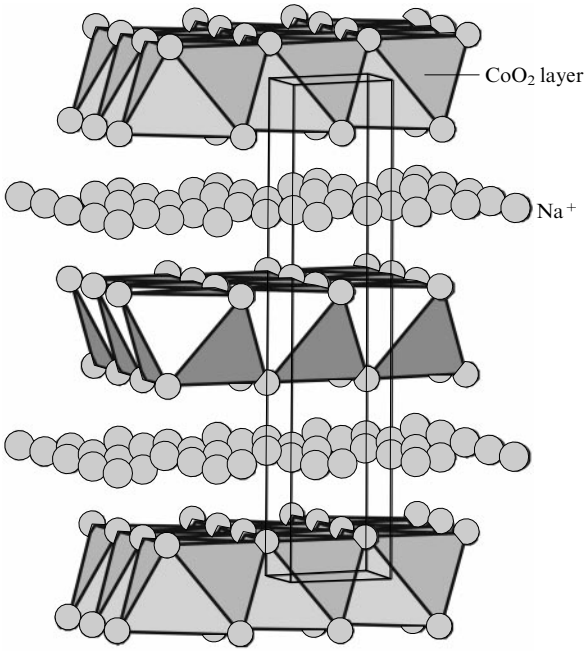


Figure 18. Crystal structure of $NaCo_2O_4$.
Alternation of edge-shared CoO_6 octahedra with the layers of sodium ions disordered over several positions.

The extraordinary properties of $NaCo_2O_4$ are determined by two peculiarities of its crystal and electron structures. First, sodium atoms are randomly distributed within the layers situated between the CoO_2 layers and have high atomic displacement parameters. Second, bonding between cobalt and oxygen atoms is essentially ionic. Thus, sodium atoms are capable of the simultaneous effective scattering of phonons and conduction electrons, which determines the relatively low thermal conductivity of this material and its anisotropic electrical conductivity. Moreover, no localisation of states was observed even at very low temperatures, which is very unusual for a 2D conductor. This suggests that $NaCo_2O_4$ represents a strongly correlated 3d-system in which the valence fluctuations (Co^{3+}/Co^{4+}) provide the high thermopower values despite the metallic conduction.[165]

The crystal structure of Na_xCoO_2 undergoes weak transformations with the varying composition. It was found [166] that the best values of thermoelectric figure-of-merit ($ZT \approx 0.8$ at

1000 K) are observed for the so-called γ-phase at $0.55 \leqslant x \leqslant 0.70$.

Other mixed cobalt oxides with advantageous thermoelectric properties include the compounds $Ca_3Co_4O_9$ and $Bi_2Sr_2CaCo_2O_8$ with the misfit (incommensurate) structures. The crystal structure of $Ca_3Co_4O_9$ consists of Ca_2CoO_3 blocks with the rock-salt structure and CoO_2 blocks with the CdI_2 structure, which are misfit. The oxide $Bi_2Sr_2CaCo_2O_8$ with the formal composition coinciding with that of a copper-containing high-temperature superconductor has an even more intricate crystal structure based on the alternating $Bi_2Sr_2O_4$ and CoO_2 blocks.[167, 168] In the oxide $Ca_3Co_4O_9$, ions Co^{2+}, Co^{3+} and Co^{4+} coexist, which leads to the manifestation of unusual magnetic and thermoelectric properties. Particularly, being an anisotropic metallic conductor, this compound demonstrated a thermopower, which approached 125 μV K^{-1} at room temperature and depended on the intensity of the applied magnetic field. Moreover, for a high thermopower value to be realised, the cobalt ions should remain in the low-spin state.[165, 169]

It should be noted that as the crystal structure of mixed cobalt oxides becomes more complicated, their thermal conductivity decreases. Thus the lowest value of thermal conductivity at room temperature ($\sim$2 W m^{-1} K^{-1}) belongs to $Bi_2Sr_2CaCo_2O_8$, which is due to the strongest structural disordering and the largest mass of disordered atoms (in this case, bismuth).[170]

VIII. Nanosized thermoelectric materials

The nanosized state of matter represents a new trend of the search for effective thermoelectric materials. Two physical phenomena underlie the use of nanosized objects. The first phenomenon is associated with the peculiarities of electronic structure of nanosized particles, which cause a decrease in the electrical conductivity but may simultaneously lead to a substantial increase in the thermopower; as a result, the power factor of a nanosized thermoelectric is higher as compared with a bulk ceramic sample. The physical reason behind these peculiarities is associated with the fact that in the nanosized state, the band gap of a semiconductor widens with the simultaneous increase in the density of states near the Fermi level. The second phenomenon is associated with the appearance of a large number of interfaces, which effectively scatter phonons but exert a minor effect on the transport of charge carriers due to the very small size of particles.[171, 172] The studies of thermoelectric properties in nanosystems are focused on the following two types of objects: the true nanosized particles, structures and superlattices and the bulk nanocomposites. As a rule, the compounds already known as the promising thermoelectric materials are employed. First of all, these are bismuth and lead tellurides, Si–Ge alloys and skutterudites.

1. Nanoparticles and nanostructures

There are different ways for the synthesis of nanoparticles of bismuth telluride Bi_2Te_3, for example, the solvothermal synthesis, the sonication-induced synthesis and electrochemical deposition. Depending on the experimental conditions, it is possible to prepare different forms of Bi_2Te_3 including hollow nanospheres, nanorods, nanobelts and nanotubes. The particle size also varies; thus the diameter of nanospheres reaches 10–50 nm, while the cross-section of nanotubes is 100–200 nm. Materials prepared by pressing of such nanoparticles demonstrated a noticeable reduction of the thermal conductivity as compared with crystalline bismuth telluride, which was explained by the appearance of an additional mechanism of phonon scattering by the interfaces of nanoparticles.[173–176]

Layered bismuth–telluride nanostructures, which were prepared by a combination of various melt techniques with spark plasma sintering, represented ordered 'nanoplates' with a thickness of 1.03 nm and a diameter of 10–40 nm. These items demonstrated the higher electrical conductivity as compared with crystalline Bi_2Te_3, which is unusual for nanoparticles and nanostructures. Insofar as their thermal conductivity is lower and the thermopower remains unchanged, the thermoelectric figure-of-merit of such a nanostructure increases up to $ZT = 1.35$ at room temperature.[177]

The hydrothermal method allows one to prepare nanoparticles of bismuth telluride doped with lanthanum. Pressed nanoparticles of the $La_{0.2}Bi_{1.8}Te_3$ composition demonstrated $ZT = 0.58$ at 480 K, which, however, is comparable with the figure-of-merit of a bulk non-doped Bi_2Te_3 sample.[178]

Thermoelectric properties of nanoparticles and nanostructures of other compounds were studied less extensively. In particular, nanoparticles of cobalt antimonide $CoSb_3$ with the skutterudite structure were synthesised by the solvothermal method in ethanol from antimony and cobalt chlorides and $NaBH_4$ as the reducing agent. The size of the synthesised particles was $\sim$150 nm and weakly depended on the temperature and the synthesis time. The comprehensive research of thermoelectric properties of such nanoparticles was never undertaken; however, it was shown[179] that the temperature dependence of the Zeebeck coefficient has a complex shape with the absolute maximum of $|-230|$ μV K^{-1} at 550 K. The synthesis of zinc antimonide Zn_4Sb_3 nanoparticles by annealing the solvothermally activated zinc and antimony powders was reported;[180] however, only preliminary data on the heat transport in this material were shown.

Carbon nanotubes proved to be an interesting subject for studying the thermoelectric properties.[181] Depending on the oxygen content, they demonstrated different types of conduction. Thus oxygen-saturated single-walled nanotubes were the p-conductors and had thermopower of $+40$ μV K^{-1} at 300 K. Deoxygenation resulted in the changeover of the dominant charge carriers to electrons, and the thermopower took a value of -60 μV K^{-1}. At the same time, the thermal conductivity of carbon nanotubes was relatively high ($\sim$5 W m^{-1} K^{-1}) and, correspondingly, their thermoelectric figure-of-merit was low.[182–184]

2. Superlattices

The development of superlattices based on already known thermoelectrics is a promising trend of the quest for thermoelectric materials. Superlattices based on bismuth telluride and selenide, antimony telluride and lead telluride were studied.

The ability of superlattices to effectively scatter phonons without impeding the transport of charge carriers was demonstrated by the example of thin-film Bi_2Te_3–Sb_2Te_3 superlattices. These epitaxial films were obtained in the deposition of Bi_2Te_3 and Sb_2Te_3 layers on a gallium arsenide substrate by the MOCVD method (Metal Organic Chemical Vapour Deposition) and had a misorientation angle of 2–4° and a repetition period of 6 nm. It was shown that a decrease in the thermal conductivity leads to a substantial increase in the thermoelectric figure-of-merit up to $ZT = 2.4$ at 300 K, which is 2.5-times higher as compared with bulk samples of the same composition.[185]

Other methods of preparation of superlattices included molecular-beam epitaxy, co-evaporation, sputtering and electrochemical deposition. These methods were used for the synthesis of PbTe–PbSe, PbTe–$PbTe_xSe_{1-x}$ and Bi_2Te_3–PbTe superlattices formed by thin films and quantum dots. For the most part, these superlattices demonstrated considerably higher values of the thermoelectric figure-or-merit as compared with ordinary crystalline compounds; for the PbTe–$PbTe_xSe_{1-x}$ superlattices, $ZT = 1.6$ at room temperature and $ZT = 2.5$ at 400 K.[186–188] In all the cases, the higher figure-of-merit values for superlattices were associated with the more effective phonon scattering. Probably, still lower thermal conductivities might be obtained on superlattices of nanowires and on aperiodic superlattices. At the same time, the mechanisms of enhancement of the power factor in superlattices were not yet enabled.[189]

Superlattices are anisoptropic and have small dimensions. A very serious problem concerns the reliable determination of their thermoelectric properties, because the conventional methods of applying contacts aimed at measuring signals and determining temperature gradients cannot be used.[190, 191] This is why it is often impossible to assess the reliability of published data on thermoelectric properties and no reproducibility was achieved in the majority of cases.

3. Nanocomposites

In contrast to superlattices, nanocomposites are bulk (massive) objects, for which the reliable measurements of properties is an 'easy' task. A thermoelectric composite represents a material with the random distribution of nanoparticles of two chemical compounds or with nanoparticles of the active component placed into a matrix of a potential thermoelectric (Fig. 19). The different principles of organisation of nanocomposites require different approaches to their synthesis. Thus distributed nanoparticles are as a rule obtained by mechanochemical methods, whereas matrix nanocomposites are obtained by the fast co-crystallisation of a matrix and an additive.[171]

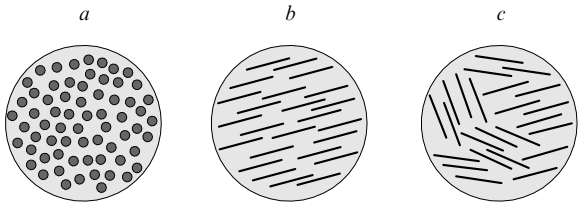


Figure 19. Schematic representation of various nanocomposites. (*a*) spherical nanoparticles in a matrix, (*b*) oriented nanorods in a matrix, (*c*) randomly oriented nanorods in a matrix.

The studies of thermoelectric properties of the Si–Ge nanocomposite (germanium and silicon nanoparticles) with particles measuring 10 and 50 nm have shown that the thermal conductivity of this material decreased with the decrease in the particle size; moreover, for a certain composition with 10-nm particles, the thermal conductivity decreased nearly five-fold (down to 1–1.5 W m^{-1} K^{-1}) and remained virtually unchanged in a temperature range of 300–1000 K.[192] By the example of a $Si_{0.8}Ge_{0.2}$ composite alloyed with boron (1.6 at.%), the simultaneous decrease in the electrical conductivity and increase in the thermopower as compared with the analogous alloy was convincingly demonstrated (Fig. 20). The relative changes in these quantities were such that the power

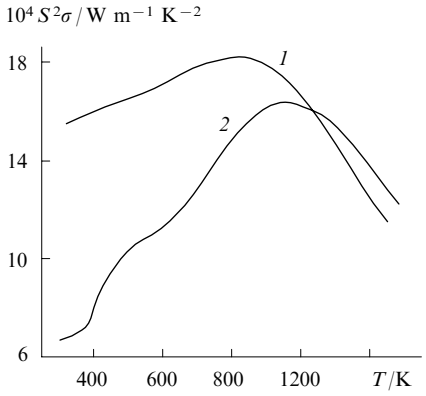


Figure 20. Power factors of (*1*) $Si_{0.8}Ge_{0.2}$ + 1.6 at.% B nanocomposite and (*2*) doped alloy of the same composition.

factor of the nanocomposite exceeded the corresponding value for the alloy; moreover, the advantages of the nanomaterial were the most pronounced at temperatures close to ambient at which the ratio of power factors was 2.5.[171]

Lead telluride was often used as a matrix in the synthesis of nanocomposites. The incorporation of the antimony or indium antimonide particles into PbTe allowed the thermal conductivity of the material at room temperature to be decreased almost threefold, *viz*., down to 0.8 W m^{-1} K^{-1}. It was noted that with the increase in the nanocomponent content, the thermal conductivity changed non-monotonically and had a minimum, which for a PbTe–Sb nanocomposite corresponded to 2 at.% antimony. These nanocomposites were also characterised by a slight increase in the thermopower as compared with the matrix material.[193, 194] Similar results were also obtained for a different nanocomposite that represented a matrix of indium and gallium arsenide $In_{0.53}Ga_{0.47}As$ with incorporated ErAs nanoparticles measuring from 1 to 4 nm. The experiments and theoretical calculations have shown that the additional contribution into the reduction of the thermal conductivity was largely due to the phonon scattering by erbium arsenide nanoparticles, which resulted in the double thermoelectric figure-of-merit of this material.[195]

Extraordinary samples were synthesised by the incorporation of Bi_2Te_3 nanotubes into a matrix of the same composition. Such 'synergistic' composites (or co-essential nanocomposites) demonstrate the properties intrinsic to neither bulk samples nor bismuth telluride nanoparticles. Due to the specific conditions of phonon scattering, the thermal conductivity of such a sample decreased down to 0.8 W m^{-1} K^{-1}. Moreover, the transport of charge carriers did not suffer any substantial changes, and the nanocomposite demonstrated the high figure-of-merit values, namely the maximum $ZT = 1.25$ was reached at 420 K.[196, 197]

IX. Conclusion

Thermoelectric materials that appeared in the late 1950s had $ZT \leqslant 1$. These materials found their application in certain fields of technology; however, their further improvement was apparently impossible. The concept 'phonon glass–electron crystal' put forward by Slack [10] in the mid-1990s served as the theoretical basis for the development of the new thermoelectric materials.

This concept pointed out the possible ways for the independent optimisation of three factors that determine the

thermoelectric figure-of-merit of a material, namely, electrical conductivity, thermopower and thermal conductivity. However, the choice of candidates for thermoelectric materials is based on the concepts of chemistry, more exactly, on the knowledge of the structure – property relationships for certain classes of compounds. The analysis of possible mechanisms of scattering of heat-carrying phonons by narrow-gap semiconductors and semimetals makes it possible to outline the circle of objects promising for the development of new thermoelectrics. Such mechanisms include scattering by rattling of atoms trapped in the cavities formed in covalently bonded frameworks, scattering by crystal-structure heterogeneities or lattice irregularities and scattering by interfaces of nanoparticles. Each of these mechanisms requires its own specific approach to the determination of candidates for thermoelectric materials. Moreover, the main requirement is that the realisation of a phonon scattering mechanism aimed at the reduction of the thermal conductivity does not impede the effective transport of charge carriers.[198]

From the chemical viewpoint, the synthesis of efficient thermoelectric materials is associated with the solution of several problems. First of all, this is the synthesis of compounds with the target structure and the controllable concentration of valence electrons. Yet another problem consists in the doping (alloying) of promising materials aimed at the optimisation of the charge carrier concentration without considerable increase in the thermal conductivity of the material. Moreover, it is necessary to develop methods for the synthesis of metastable compounds, including nanoparticles of a given size, ordered nanostructures and nanocomposites. Finally, the search for new classes of thermoelectric materials based on their predicted structures and possible properties is still of current importance. The solution of this problem involves not only the quest for new types of crystal structures (*e.g.*, the recent synthesis[199] of $CrAuTe_4$ with the promising thermoelectric properties), but also the studies of properties of already known compounds the crystal and electron structures of which favour the manifestation of the desired properties.[200]

At present, the development of thermoelectric materials that demonstrate the figure-of-merit values higher than those of commercially available thermoelectrics at least at temperatures below 500 K can be considered as the already solved problem. In the middle temperature range (500 – 800 K), these materials include several members of the LAST family, zinc antimonide Zn_4Sb_3 and certain filled skutterudites. For higher temperatures, the best characteristics belong to $Yb_{14}MnSb_{11}$.

Advances in the development of nanomaterials with promising thermoelectric properties are evident: $ZT = 2.4$ are achieved. Of no lesser importance is the search for materials capable of low-temperature operation in a combination with semiconductors. Such materials can be found among heavily doped semimetals and degenerate semiconductors of which many exhibit the high electrical conductivity that, at low temperatures, can compensate their relatively low thermopower. One should not rule out the prospects for the synthesis of new, in principle, substances with the record properties that would allow one to approach the thermoelectric figure-of-merit $ZT = 3$.

The interest of the scientific community in the problem under discussion was reflected in the growth in publications devoted to the quest for new thermoelectric materials. Thus in 2006, nearly 900 original papers on the synthesis and investigation of thermoelectric materials were published, which is nearly four times higher as compared with 1995 when a collection of papers was published[201] that covered all the aspects of this problem and specified the new research direction based on the PGEC concept.

The author is grateful to Dr. K A Kovnir (Max-Plank Institute, Dresden, Germany) and Prof. M M Shatruk (Florida State University, Tallahassee) for the discussion of various aspects of the subject under consideration.

This review was prepared with the financial support of the Russian Foundation for Basic Research (Project Nos 06-03-32183 and 07-03-12155).

References

1. N Armaroli, V Balzani *Angew. Chem., Int. Ed.* **46** 52 (2007)
2. H J Goldshmid *Electronic Refrigeration* (London: Pion Ltd, 1986)
3. B C Sales *Curr. Opin. Solid State Mater. Sci.* **2** 284 (1997)
4. A V Shevelkov *Vestn. Mosk. Univ., Ser. Khim.* **44** 163 (2003) [a]
5. T M Tritt, M A Subramanian *MRS Bull.* **31** 188 (2006)
6. M A White *Properties of Materials* (New York: Oxford University Press, 1999)
7. F J DiSalvo *Science* **285** 703 (1999)
8. A F Ioffe *Semiconductor Thermoelements and Thermoelectric Cooling* (London: Infosearch Ltd, 1957)
9. N Kh Abrikosov, V F Bankina *Zh. Neorg. Khim.* **3** 659 (1958) [b]
10. G S Nolas, J Sharp, H J Goldsmid *Thermoelectrics: Basic Principles and New Materials Developments* (New York: Springer, 2001)
11. T S Kim, B S Chun, J K Lee, H G Jung *J. Alloys Compd.* **434 – 435** 710 (2007)
12. M Carle, P Pierrat, C Lahalle-Gravier, S Scherrer, H Scherrer *J. Phys. Chem. Solids* **56** 201 (1995)
13. J Yang, T Aizawa, A Yamamoto, T Ohta *J. Alloys Compd.* **309** 225 (2000)
14. J L Cui, W J Xiu, L D Mao, P Z Ying, L Jiang, X Qian *J. Solid State Chem.* **180** 1158 (2007)
15. J L Cui, H F Xue, W J Xiu, L Jiang, P Z Ying *J. Solid State Chem.* **179** 3751 (2006)
16. S S Kim, F Yin, Y Kagawa *J. Alloys Compd.* **419** 306 (2006)
17. X A Fan, J Y Yang, W Zhu, H S Yun, R G Chen, S Q Bao, X K Duan *J. Alloys Compd.* **420** 256 (2006)
18. S Ahmad, K Hoang, S D Mahanti *Phys. Rev. Lett.* **96** 056403 (2006)
19. P Zhu, Y Imai, Y Isoda, Y Shinohara, X Jia, G Zou *J. Phys. Condens. Matter* **17** 7319 (2005)
20. Y Gelbstein, Z Dashevsky, M P Dariel *Physica B* **363** 196 (2005)
21. Y Gelbstein, Z Dashevsky, M P Dariel *Physica B* **391** 256 (2007)
22. M Orihashi, Y Noda, L D Chen, T Goto, T Hirai *J. Phys. Chem. Solids* **61** 919 (2000)
23. P Zhu, Y Imai, Y Isoda, Y Shinohara, X Jia, G Zou *J. Alloys Compd.* **420** 233 (2006)
24. Z H Dughaish *Physica B* **322** 205 (2002)
25. C Wood *Rep. Prog. Phys.* **51** 459 (1988)
26. T Baba, T Ilida, H Hirahara, T Itoh, M Akasaka, Y Takanashi *Mater. Res. Soc. Symp. Proc.* **886** 449 (2006)
27. M Otake, K Sato, O Sygiyama, S Kaneko *Solid State Ionics* **172** 523 (2004)
28. A Druzhinin, I Ostrovskii, I Kogut *Mater. Sci. Semicond. Proc.* **9** 853 (2006)
29. N S Golovanova, V P Zlomanov, O I Tananaeva *Izv. Akad. Nauk SSSR, Neorg. Mater.* **19** 740 (1983) [c]
30. A G Talybov, B K Vainshtein *Kristallografiya* **7** 43 (1962) [d]
31. L A Kuznetsova, V L Kuznetsov, D M Rowe *J. Phys. Chem. Solids* **61** 1269 (2000)
32. L E Shelimova, O G Karpinskii, P P Konstantinov, E S Avilov, M A Kretova, V S Zemskov *Izv. Akad. Nauk, Neorg. Mater.* **40** 451 (2004) [c]
33. L E Shelimova, P P Konstantinov, O G Karpinskii, E S Avilov, M A Kretova, V S Zemskov *Izv. Akad. Nauk, Neorg. Mater.* **40** 1146 (2004) [c]

34. L E Shelimova, P P Konstantinov, O G Karpinsky, E S Avilov, M A Kretova, V S Zemskov *J. Alloys Compd.* **329** 50 (2001)
35. D-Y Chung, T Hogan, P Brazis, M Rocci-Lane, C R Kannewurf, M Bastea, C Uher, M G Kanatzidis *Science* **287** 1024 (2000)
36. P Larson, S D Mahanti, D-Y Chung, M G Kanatzidis *Phys. Rev., Sect. B* **65** 045205 (2002)
37. D -Y Chung, T P Hogan, M Rocci-Lane, P Brazis, J R Ireland, C R Kannewurf, M Bastea, C Uher, M G Kanatzidis *J. Am. Chem. Soc.* **126** 6414 (2004)
38. K-F Hsu, D-Y Chung, S Lal, A Mrotzek, T Kyratsi, T Hogan, M G Kanatzidis *J. Am. Chem. Soc.* **124** 2410 (2002)
39. A Assoud, S Thomas, B Sutherland, H Zhang, T M Tritt, H Kleinke *Chem. Mater.* **18** 3866 (2006)
40. T Kyratsi, M G Kanatzidis *Z. Anorg. Allg. Chem.* **629** 2222 (2003)
41. T Kyratsi, E Hatzikraniotis, K M Paraskevopoulos, C D Malliakas, J S Dyck, C Uher, M G Kanatzidis *J. Appl. Phys.* **100** 123704 (2006)
42. Yu D Tretyakov, L I Martynenko, A N Grigor'ev, A Yu Tsivadze *Neorganicheskaya Khimiya. Khimiya Elementov* (Inorganic Chemistry. The Chemistry of Elements) (2nd-Ed.) (Moscow: Moscow State University, 2007) Ch. 3
43. M B Babanly, Z A Guseinov *Z. Metallkd.* **92** 451 (2001)
44. J W Sharp, B C Sales, D G Mandrus *Appl. Phys. Lett.* **74** 3794 (1999)
45. T Doert, P Böttcher *Z. Kristallogr.* **209** 95 (1994)
46. S Yamanaka, A Kosuga, K Kurosaki *J. Alloys Compd.* **352** 275 (2003)
47. B Wölfing, C Kloc, J Teubner, E Bucher *Phys. Rev. Lett.* **86** 4350 (2001)
48. K Kurosaki, A Kosuga, H Muta, S Yamanaka *Mater. Trans.* **46** 1502 (2005)
49. K Kurosaki, A Kosuga, H Muta, M Uno, S Yamanaka *Appl. Phys. Lett.* **87** 1 (2005)
50. K Kurosaki, A Kosuga, K Goto, H Muta, S Yamanaka *Mater. Trans.* **47** 1938 (2006)
51. M A McGuire, T K Reynolds, F J DiSalvo *Chem. Mater.* **17** 2875 (2005)
52. M A McGuire, T K Reynolds, F J DiSalvo *J. Alloys Compd.* **425** 81 (2006)
53. M A McGuire, T J Scheidemantel, J V Badding, F J DiSalvo *Chem. Mater.* **17** 6186 (2005)
54. F Rieger, A V Mudring *Chem. Mater.* **19** 221 (2007)
55. G A Slack, in *CRC Handbook of Thermoelectrics* (Ed. D M Rowe) (Boca Raton, FL: CRC Press, 1995) p. 407
56. N Mandel, J Donohue *Acta Crystallogr., Sect. B* **27** 2288 (1971)
57. D J Braun, W Jeitschko *J. Solid State Chem.* **32** 357 (1980)
58. W Jeitschko, D J Braun *Acta Crystallogr., Sect. B* **33** 3401 (1977)
59. G S Nolas, D T Morelli, T M Tritt *Annu. Rev. Mater. Sci.* **29** 89 (1999)
60. M Llunell, P Alemany, S Alvarez, V P Zhukov, A Vernes *Phys. Rev. B* **53** 10605 (1996)
61. B C Sales, D Mandrus, R K Williams *Science* **272** 1325 (1996)
62. B C Sales, D Mandrus, B C Chakoumakos, V Keppens, J R Thompson *Phys. Rev. B* **56** 15081 (1997)
63. A A Gippius, E N Morozova, K S Okhotnikov, E A Alkaev, A V Shevelkov, M Baenitz, A Leithe-Jasper, H Rosner, R Viennois, Y Grin, F Steglich *Physica B* **378**–**380** 239 (2006)
64. D T Morelli, G P Meisner, B Chen, S Hu, C Uher *Phys. Rev. B* **56** 7376 (1997)
65. G S Nolas, M Kaeser, R Littleton IV, T M Tritt *Appl. Phys. Lett.* **77** 1822 (2000)
66. J S Dyck, W Chen, C Uher, L Chen, X Tang, T Hirai *J. Appl. Phys.* **91** 3698 (2002)
67. A P Grosvenor, R G Cavell, A Mar *Chem. Mater.* **18** 1650 (2006)
68. A Leithe-Jasper, W Schnelle, H Rosner, M Baenitz, A Rabis, A A Gippius, E N Morozova, H Borrmann, U Burkhardt, R Ramlau, U Schwarz, J A Mydosh, Y Grin, V Ksenofontov, S Reiman *Phys. Rev. B* **70** 214418 (2004)
69. K Matsuhira, C Sekine, K Kihou, I Shirotani, M Wakeshima, Y Hinatsu, Y Sei, A Nakamura, S Takagi *Physica B* **378**–**380** 235 (2006)
70. X Tanga, Q Zhang, L Chen, T Goto, T Hirai *J. Appl. Phys.* **97** 093712 (2005)
71. R C Mallik, J-Y Jung, V Damodara-Das, S-C Ur, I-H Kim *Solid State Commun.* **141** 233 (2007)
72. P Vaqueiro, G G Sobany, A V Powell, K S Knight *J. Solid State Chem.* **179** 2047 (2006)
73. J W G Bos, R J Cava *Solid State Commun.* **141** 38 (2007)
74. T Caillat, A Borshchevsky, J-P Fleurial *J. Appl. Phys.* **80** 4442 (1996)
75. A Wells *Structural Inorganic Chemistry* (Oxford: Clarendon Press, 1984)
76. J Dünner, A Mewis *Z. Anorg. Allg. Chem.* **621** 191 (1995)
77. K A Kovnir, A V Shevelkov *Usp. Khim.* **73** 999 (2004) [*Russ. Chem. Rev.* **73** 923 (2004)]
78. S Bobev, S C Sevov *J. Solid State Chem.* **153** 92 (2000)
79. J V Zaikina, K A Kovnir, A V Sobolev, I A Presniakov, Y Prots, M Baitinger, W Schnelle, A V Olenev, O I Lebedev, G Van Tendeloo, Y Grin, A V Shevelkov *Chem.–Eur. J.* **13** 5090 (2007)
80. K Kishimoto, S Arimura, T Koyanagi *Appl. Phys. Lett.* **88** 222115 (2006)
81. S Paschen, W Carrillo-Cabrera, A Bentien, V H Tran, M Baenitz, Y Grin, F Steglich *Phys. Rev. B* **64** 214404 (2001)
82. B C Sales, B C Chakoumakos, R Jin, J R Thompson, D Mandrus *Phys. Rev. B* **63** 245113 (2001)
83. J V Zaikina, W Schnelle, K A Kovnir, A V Olenev, Y Grin, A V Shevelkov *Solid State Sci.* **9** 664 (2007)
84. B C Sales, B C Chakoumakos, D Mandrus, J W Sharp *J. Solid State Chem.* **146** 528 (1999)
85. G S Nolas, B C Chakoumakos, B Mahieu, G J Long, T J R Weakley *Chem. Mater.* **12** 1947 (2000)
86. S Paschen, V Pacheco, A Bentien, A Sanchez, W Carrillo-Cabrera, M Baenitz, B B Iversen, Y Grin, F Steglich *Physica B* **328** 39 (2003)
87. M M Shatruk, K A Kovnir, A V Shevelkov, I A Presniakov, B A Popovkin *Inorg. Chem.* **38** 3455 (1999)
88. K A Kovnir, J V Zaikina, L N Reshetova, A V Olenev, E V Dikarev, A V Shevelkov *Inorg. Chem.* **43** 3230 (2004)
89. C Gatti, L Bertini, N P Blake, B B Iversen *Chem.–Eur. J.* **9** 4556 (2003)
90. M M Shatruk, K A Kovnir, M Lindsjl, I A Presniakov, L A Kloo, A V Shevelkov *J. Solid State Chem.* **161** 233 (2001)
91. G J Miller, in *Chemistry, Structure, and Bonding of Zintl Phases and Ions* (Ed. S M Kauzlarich) (New York: VCH, 1996) p. 1
92. A V Shevelkov, M M Shatruk *Izv. Akad. Nauk, Ser. Khim.* 337 (2001) [c]
93. N P Blake, D Bryan, S Latturner, L Møllnitz, G D Stucky, H Metiu *J. Chem. Phys.* **114** 10063 (2001)
94. K Moriguchi, S Munetoh, A Shintani, T Motooka *Phys. Rev. B* **64** 195409 (2001)
95. K A Kovnir, M M Shatruk, L N Reshetova, I A Presniakov, E V Dikarev, M Baitinger, F Haarmann, W Schnelle, M Baenitz, Y Grin, A V Shevelkov *Solid State Sci.* **7** 957 (2005)
96. K A Kovnir, A V Sobolev, I A Presniakov, O I Lebedev, G Van Tendeloo, W Schnelle, Y Grin, A V Shevelkov *Inorg. Chem.* **44** 8786 (2005)
97. C L Condron, J Martin, G S Nolas, P M B Piccoli, A J Schultz, S M Kauzlarich *Inorg. Chem.* **45** 9381 (2006)
98. A Bentien, V Pacheco, S Paschen, Y Grin, F Steglich *Phys. Rev. B* **71** 165206 (2005)
99. V L Kuznetsov, L A Kuznetsova, A E Kaliazin, D M Rowe *J. Appl. Phys.* **87** 1 (2000)
100. M Beekman, G S Nolas *Physica B* **383** 111 (2006)
101. A M Guloy, R Ramlau, Z Tang, W Schnelle, M Baitinger, Y Grin *Nature (London)* **443** 320 (2006)
102. T Caillat, J-P Fleurial, A Borshchevsky *J. Phys. Chem. Solids* **58** 1119 (1997)
103. F Cargnoni, E Nishibori, P Rabiller, L Bertini, G J Snyder, M Christensen, C Gatti, B B Iversen *Chem.–Eur. J.* **10** 3861 (2004)
104. K-F Hsu, S Loo, F Guo, W Chen, J S Dyck, C Uher, T Hogan, E K Polychroniadis, M G Kanatzidis *Science* **303** 818 (2004)

105. A Kosuga, M Uno, K Kurosaki, S Yamanaka *J. Alloys Compd.* **387** 52 (2005)
106. A Kosuga, M Uno, K Kurosaki, S Yamanaka *J. Alloys Compd.* **391** 288 (2005)
107. A Kosuga, K Kurosaki, H Muta, S Yamanaka *J. Alloys Compd.* **416** 218 (2006)
108. D Bilc, S D Mahanti, E Quarez, K-F Hsu, R Pcionek, M G Kanatzidis *Phys. Rev. Lett.* **93** 146403 (2006)
109. D Bilc, S D Mahanti, M G Kanatzidis *Phys. Rev. B* **74** 125202 (2006)
110. E Quarez, K-F Hsu, R Pcionek, N Frangis, E K Polychroniadis, M G Kanatzidis *J. Am. Chem. Soc.* **127** 9177 (2005)
111. P F P Poudeu, J D'Angelo, A D Downey, J L Short, T P Hogan, M G Kanatzidis *Angew. Chem., Int. Ed.* **45** 3835 (2006)
112. S K Plachkova, I A Avramova *Phys. Status Solidi, A* **184** 195 (2001)
113. S K Plachkova *Phys. Status Solidi, A* **83** 349 (1984)
114. Y Mozharivskyj, Y Janssen, J L Harringa, A Kracher, A O Tsokol, G J Miller *Chem. Mater.* **18** 822 (2006)
115. J Nylén, S Lidin, M Andersson, B B Iversen, H Liu, N Newman, U Häussermann *Chem. Mater.* **19** 834 (2007)
116. G J Snyder, M Christensen, E Nishibori, T Caillat, B B Iversen *Nature Mater.* **3** 458 (2004)
117. J Nylén, M Andersson, S Lidin, U Hiussermann *J. Am. Chem. Soc.* **126** 16306 (2004)
118. Y Mozharivskyj, A O Pecharsky, S Bud'ko, G J Miller *Chem. Mater.* **16** 1580 (2004)
119. A S Mikhaylushkin, J Nylén, U Hiussermann *Chem. – Eur. J.* **11** 4912 (2005)
120. S G Kim, I I Mazin, D J Singh *Phys. Rev. B* **57** 6199 (1998)
121. K Ueno, A Yamamoto, T Noguchi, C H Li, T Inoue, S Sodeoka, H Obara *J. Alloys Compd.* **417** 259 (2006)
122. O Y Zelinska, H Bie, A Mar *Chem. Mater.* **19** 1518 (2007)
123. N A Ignat'ev, Ya A Ugai, K B Aleinikova, N S Rabotkina *Zh. Neorg. Khim.* **12** 729 (1971) [b]
124. V Ya Shevchenko, G I Goncharenko, V F Dvoryankin, Ya A Ugai, T A Marshakova *Izv. Akad. Nauk SSSR, Neorg. Mater.* **2** 312 (1971) [c]
125. V L Kuznetsov, D M Rowe *J. Alloys Compd.* **372** 103 (2004)
126. R Viennois, M-C Record, V Izard, J-C Tedenac *J. Alloys Compd.* **440** L22 (2007)
127. S M Kauzlarich, S R Brown, G J Snyder *Dalton Trans.* 2099 (2007)
128. H Nowotny, W Sibert *Z. Metallkd.* **33** 391 (1941)
129. S Ogut, K M Rabe *Phys. Rev. B* **51** 10443 (1995)
130. P Larson, S D Mahanti, S Sportouch, M G Kanatzidis *Phys. Rev. B* **59** 15660 (1999)
131. I Galanakis, P H Dederichs, N Papanikolaou *Phys. Rev. B* **66** 134428 (2002)
132. S Bhattacharya, A L Pope, R T Littleton IV, T M Tritt, V Ponnambalam, Y Xia, S J Poon *Appl. Phys. Lett.* **77** 2476 (2000)
133. F G Aliev, N B Brandt, V V Moschalkov, V V Kozyrkov, R V Skolozdra, A I Belogorokhov *Z. Phys. B: Condens. Matter* **80** 353 (1990)
134. S Katsuyama, R Matsuo, M Ito *J. Alloys Compd.* **428** 262 (2007)
135. K Kurosaki, H Muta, S Yamanaka *J. Alloys Compd.* **384** 149 (2004)
136. Q Shen, L Chen, T Goto, T Hirai, J Yang, G P Meisner, C Uher *Appl. Phys. Lett.* **79** 4165 (2001)
137. G Cordier, H Schäfer, M Stelter *Z. Anorg. Allg. Chem.* **519** 183 (1984)
138. A P Holm, T C Ozawa, S M Kauzlarich, S A Morton, G D Waddill, J G Tobin *J. Solid State Chem.* **178** 262 (2005)
139. A P Holm, S M Kauzlarich, S A Morton, G D Waddill, W E Pickett, J G Tobin *J. Am. Chem. Soc.* **124** 9894 (2002)
140. S R Brown, S M Kauzlarich, F Gascoin, G J Snyder *Chem. Mater.* **18** 1873 (2006)
141. C Pfleiderer, R Vollmer, M Uhlarz, A Faisst, H Von Löhneysen, A Natrepov *Physica B* **312** 352 (2002)
142. A Mewis *Z. Naturforsch., B* **33** 382 (1978)
143. F Gascoin, S Ottensmann, D Stark, S M Haïle, G J Snyder *Adv. Funct. Mater.* **15** 1860 (2005)
144. A E Dwight *Acta Crystallogr., Sect. B* **33** 1579 (1977)
145. P Larson, S D Mahanti, J Salvador, M G Kanatzidis *Phys. Rev. B* **74** 035111 (2006)
146. M Wang, R McDonald, A Mar *Inorg. Chem.* **38** 3435 (1999)
147. D Young, K Mastronardi, P Khalifah, C-C Wang, R J Cava, A P Ramirez *Appl. Phys. Lett.* **74** 3999 (1999)
148. K Mastronardi, D Young, C-C Wang, A P Ramirez, P Khalifah, R J Cava *Appl. Phys. Lett.* **74** 1415 (1999)
149. K Schubert, H Pfisterer *Z. Metallkd.* **41** 433 (1950)
150. U Häussermann, M Elding-Pontgn, C Svensson, S Lidin *Chem. – Eur. J.* **4** 1007 (1998)
151. E Dashjav, A Szczepenowska, H Kleinke *J. Mater. Chem.* **12** 345 (2002)
152. F Gascoin, J Rasmussen, G J Snyder *J. Alloys Compd.* **427** 324 (2007)
153. H Fjellvag, A Kjekshus *Solid State Commun.* **60** 91 (1986)
154. N Soheilnia, K M Kleinke, H Kleinke *Chem. Mater.* **19** 1482 (2007)
155. R T Littleton IV, T M Tritt, J W Kolis, D R Ketchum *Phys. Rev. B* **60** 13453 (1999)
156. B M Zawilski, R T Littleton IV, T M Tritt *Appl. Phys. Lett.* **77** 2319 (2000)
157. Z Fisk, D W Hess, C J Pethick, D Pines, J L Smith, J D Thompson, J O Willis *Science* **239** 33 (1988)
158. U Walter, E Holland-Moritz, Z Fisk *Phys. Rev. B* **43** 320 (1991)
159. D M Rowe, V L Kuznetsov, L A Kuznetsova, G Min *J. Phys. D* **35** 2183 (2002)
160. J R Thompson, S T Seula, C-K Loong, C Stassis *J. Appl. Phys.* **53** 7893 (1982)
161. C D W Jones, K A Regan, F J DiSalvo *Phys. Rev. B* **58** 16058 (1998)
162. M Jansen, R Hoppe *Z. Anorg. Allg. Chem.* **408** 104 (1974)
163. C Fouassier, G Matejka, P J Reau, J Hagenmüller *J. Solid State Chem.* **6** 532 (1973)
164. I Terasaki, Y Sasago, K Uchinokura *Phys. Rev. B* **56** 12685 (1997)
165. W Koshibae, K Tsutsui, S Maekawa *Phys. Rev. B* **62** 6869 (2000)
166. K Takada, H Sakurai, E Takayama-Muromachi, F Izumi, R A Dilanian, T Sasaki *Nature (London)* **422** 53 (2003)
167. A C Masset, C Michel, A Maignan, M Hervieu, O Toulemonde, F Studer, B Raveau *Phys. Rev. B* **62** 166 (2000)
168. M Hervieu, P Boullay, C Michel, A Maignan, B Raveau *J. Solid State Chem.* **142** 305 (1999)
169. N Créon, O Perez, J Hadermann, Y Klein, S Hgbert, M Hervieu, B Raveau *Chem. Mater.* **18** 5355 (2006)
170. A Satake, H Tanaka, T Ohkawa, T Fujii, I Terasaki *J. Appl. Phys.* **96** 931 (2004)
171. M S Dresselhaus, G Chen, M Y Tang, R G Yang, H Lee, D Z Wang, Z F Ren, J-P Fleurial, P Gogna *Adv. Mater.* **19** 1043 (2007)
172. N Mingo, D A Broido *J. Appl. Phys.* **101** 014322 (2007)
173. Y Y Zheng, T J Zhu, X B Zhao, J P Tu, G S Cao *Mater. Lett.* **59** 2886 (2005)
174. X B Zhao, X H Ji, Y H Zhang, B H Lu *J. Alloys Compd.* **368** 349 (2004)
175. M Martin-Gonzalez, G J Snyder, A L Prieto, R Gronsky, T Sands, A M Stacy *Nano Lett.* **3** 973 (2003)
176. W Z Wang, B Poudel, Y Ma, Z F Ren *J. Phys. Chem. B* **110** 25702 (2006)
177. X Tang, W Xie, H Li, W Zhao, Q Zhang, M Niino *Appl. Phys. Lett.* **90** 012102 (2007)
178. Y H Zhang, T J Zhu, J P Tu, X B Zhao *Mater. Chem. Phys.* **103** 484 (2007)
179. J L Mi, X B Zhao, T J Zhu, J P Tu, G S Cao *J. Alloys Compd.* **417** 269 (2006)
180. S Schlecht, C Erk, M Yosef *Inorg. Chem.* **45** 1693 (2006)
181. S Iijima *Nature (London)* **354** 56 (1991)
182. P G Collins, K Bradley, M Ishigami, A Zettl *Science* **287** 1801 (2000)

183. K McGuire, N Gothard, P L Gai, M S Dresselhaus, G Sumanasekera, A M Rao *Carbon* **43** 219 (2005)
184. H L Zhang, J-F Li, K F Yao, L D Chen *J. Appl. Phys.* **97** 1 (2005)
185. R Venkatasubramanian, E Siivola, T Colpitts, B O'Quinn *Nature (London)* **413** 597 (2001)
186. B Yoo, F Xiao, K N Bozhilov, J Herman, M A Rayan, N V Myung *Adv. Mater.* **19** 296 (2007)
187. T C Harman, P Taylor, M P Walsh, B E LaForge *Science* **297** 2229 (2002)
188. G Springholz, V Holy, M Pinczolits, G Bauer *Science* **282** 734 (1998)
189. Y-M Lin, M S Dresselhaus *Phys. Rev. B* **60** 075304 (2003)
190. W S Capinski, H J Maris, T Ruf, M Cardona, K Ploog, D S Katzer *Phys. Rev. B* **59** 8105 (1999)
191. D G Cahill, W K Ford, K E Goodson, G D Mahan, A Majumdar, H J Maris, R Merlin, S R Phillpot *J. Appl. Phys.* **93** 793 (2003)
192. R Yang, G Chen *Phys. Rev. B* **69** 195316 (2004)
193. J R Sootsman, R J Pcionek, H Kong, C Uher, M G Kanatzidis *Chem. Mater.* **18** 4993 (2006)
194. J P Heremans, C M Thrush, D T Morelli *Phys. Rev. B* **70** 115334 (2004)
195. W Kim, J Zide, A Gossard, D Klenov, S Stemmer, A Shakouri, A Majumdar *Phys. Rev. Lett.* **96** 045901 (2006)
196. X B Zhao, X H Ji, Y H Zhang, T J Zhu, J P Tu, X B Zhang *Appl. Phys. Lett.* **86** 062111 (2005)
197. X H Ji, X B Zhao, Y H Zhang, B H Lu, H L Ni *J. Alloys Compd.* **387** 282 (2005)
198. G S Nolas, J Poon, M G Kanatzidis *MRS Bull.* **31** 199 (2006)
199. T K Reynolds, M A McGuire, F J DiSalvo *J. Solid State Chem.* **177** 2998 (2004)
200. T Caillat, J-P Fleurial, G J Snyder *Solid State Sci.* **1** 535 (1999)
201. *CRC Handbook on Thermoelectrics* (Ed. D M Rowe) (Boca Raton, FL: CRC Press, 1995)

[a] — *Moscow Univ. Bull., Ser. Chem. (Engl. Transl.)*
[b] — *Russ. J. Inorg. Chem. (Engl. Transl.)*
[c] — *Inorg. Mater. (Engl. Transl.)*
[d] — *Crystallogr. Rep. (Engl. Transl.)*
[e] — *Russ. Chem. Bull., Int. Ed. (Engl. Transl.)*